AMERICAN SOCIETY FOR MICROBIOLOGY | Molecular and Cellular Biology®

RESEARCH ARTICLE

TRAF2 Ser-11 Phosphorylation Promotes Cytosolic Translocation of the CD40 Complex To Regulate Downstream Signaling Pathways

Lauren M. Workman,[a] Laiqun Zhang,[a] Yumei Fan,[a,b] Weizhou Zhang,[a] Hasem Habelhah[a]

[a]Department of Pathology, University of Iowa Carver College of Medicine, Iowa City, Iowa, USA

[b]Key Laboratory of Animal Physiology, Biochemistry and Molecular Biology of Hebei Province, College of Life Science, Hebei Normal University, Shijiazhuang, People's Republic of China

Lauren M. Workman and Laiqun Zhang contributed equally to this work, and author order was determined both alphabetically and in order of increasing seniority.

ABSTRACT CD40 plays an important role in immune responses by activating the c-Jun N-terminal protein kinase (JNK) and NF-κB pathways; however, the precise mechanisms governing the spatiotemporal activation of these two signaling pathways are not fully understood. Here, using four different TRAF2-deficient cell lines (A20.2J, CH12.LX, HAP1, and mouse embryonic fibroblasts [MEFs]) reconstituted with wild-type or phosphorylation mutant forms of TRAF2, along with immunoprecipitation, immunoblotting, gene expression, and immunofluorescence analyses, we report that CD40 ligation elicits TANK-binding kinase 1 (TBK1)-mediated phosphorylation of TRAF2 at Ser-11. This phosphorylation interfered with the interaction between TRAF2's RING domain and membrane phospholipids and enabled translocation of the TRAF2 complex from CD40 to the cytoplasm. We also observed that this cytoplasmic translocation is required for full activation of the JNK pathway and the secondary phase of the NF-κB pathway. Moreover, we found that in the absence of Ser-11 phosphorylation, the TRAF2 RING domain interacts with phospholipids, leading to the translocation of the TRAF2 complex to lipid rafts, resulting in its degradation and activation of the noncanonical NF-κB pathway. Thus, our results provide new insights into the CD40 signaling mechanisms whereby Ser-11 phosphorylation controls RING domain-dependent subcellular localization of TRAF2 to modulate the spatiotemporal activation of the JNK and NF-κB pathways.

KEYWORDS TRAF2, phosphorylation, CD40, JNK, NF-κB, signaling mechanisms

CD40 (TNFRSF5) is a member of the tumor necrosis factor receptor (TNFR) superfamily that regulates several facets of the adaptive immune response, including T cell-dependent B cell activation, germinal center (GC) formation, memory B cell development, and the generation of high-affinity, class-switched antibodies (1). Mice deficient in either CD40 or its cognate ligand CD40L (also known as CD154 or gp39), as well as humans with CD40L-inactivating mutations, exhibit hyper-IgM immunodeficiency syndrome, which is characterized by elevated serum IgM levels accompanied by an underproduction of IgA, IgG, and IgE attributed to defective class switch recombination (2).

TNFR superfamily members lack intrinsic kinase activity and must recruit one or more members of the TNFR-associated factor (TRAF) family to initiate downstream signal transduction. Six classical TRAFs have been identified and are characterized by a highly homologous C-terminal TRAF domain consisting of a coiled-coil TRAF N domain that mediates TRAF homo- and heterotrimerization and a β-sandwich TRAF C domain that interacts with receptors and other effector proteins (3). With the exception of

Citation Workman LM, Zhang L, Fan Y, Zhang W, Habelhah H. 2020. TRAF2 Ser-11 phosphorylation promotes cytosolic translocation of the CD40 complex to regulate downstream signaling pathways. Mol Cell Biol 40:e00429-19. https://doi.org/10.1128/MCB.00429-19.

Address correspondence to Hasem Habelhah, hasem-habelhah@uiowa.edu.

Received 7 September 2019
Returned for modification 14 November 2019
Accepted 29 January 2020
Accepted manuscript posted online 10 February 2020
Published 13 April 2020

TRAF1, TRAFs contain an N-terminal RING domain. A variety of cell culture experiments suggest that the RING domains of TRAF2 and TRAF6 catalyze noncanonical K63-linked polyubiquitination to activate the classical IκB kinase (IKK) complex, consisting of IKKα, IKKβ, and IKKγ subunits (4–6). However, conclusive evidence for *bona fide* E3 ligase activity by purified proteins has been demonstrated only for TRAF6 (7, 8). Notably, reconstitution of TRAF2- or TRAF2/TRAF5 (TRAF2/5)-deficient mouse embryonic fibroblasts (MEFs) with a RING domain deletion mutation of TRAF2 (TRAF2-ΔR) fully restores immediate tumor necrosis factor alpha (TNF-α)-induced NF-κB activation while only partially restoring c-Jun N-terminal protein kinase (JNK) activation (9, 10). Thus, the exact role of the TRAF2 RING domain in NF-κB and JNK activation still remains elusive.

Ligated CD40 recruits TRAF2, TRAF3, and TRAF6 through its conserved TRAF-binding sites in the cytoplasmic domain, resulting in activation of the canonical (e.g., the RelA/p50 dimer) and noncanonical (e.g., the RelB/p52 dimer) NF-κB pathways, as well as the mitogen-activated protein kinase (MAPK; e.g., JNK) cascade (11). TRAF2 and TRAF6 positively regulate CD40-induced MAPK and canonical NF-κB activation, while TRAF2 and TRAF3 negatively regulate noncanonical NF-κB. Under unstimulated conditions, an E3 ligase complex consisting of TRAF2, TRAF3, and cellular inhibitor of apoptosis 1 and 2 (cIAP1/2) constitutively targets NF-κB-inducing kinase (NIK) for ubiquitination and degradation to suppress noncanonical NF-κB activation (12, 13). Upon stimulation, the recruitment of the E3 ligase complex to CD40 elicits TRAF2/cIAP1/2-mediated ubiquitination and degradation of TRAF3 within the complex, resulting in NIK protein accumulation and NIK-dependent activation of the IKKα homodimer. IKKα then directly phosphorylates p100 to trigger its ubiquitination and proteasome-dependent partial processing to p52, allowing the nuclear translocation of the transcriptionally active RelB/p52 dimer (12, 13).

CD40 ligation has also been shown to activate phosphoinositide 3-kinase (PI3K), phospholipase Cγ (PLCγ), and Janus family kinase 3 (Jak3), but the best-characterized signaling pathways are the JNK and canonical and noncanonical NF-κB pathways. However, the spatiotemporal control of activation of these pathways is not fully understood (11). Recently, Matsuzawa et al. reported that CD40-induced JNK activation requires degradation of TRAF3 and MEKK1-mediated phosphorylation of a protein within the CD40 complex, which triggers translocation of the effector complex (consisting of MEKK1, TRAF2, cIAP1/2, and IKKγ) from CD40 to the cytoplasm, where MEKK1 is able to interact with and activate the MEK4/7-JNK cascade (14). However, several earlier studies have shown that inhibition of TRAF2 and/or TRAF3 degradation promotes JNK activation rather than inhibition (15–19). In addition, it is not known how phosphorylation of a protein within the CD40 complex triggers the translocation of the effector complex from CD40 to the cytoplasm. Notably, Chaudhuri et al. reported that CD40 signaling elicits TRAF2 phosphorylation on serine residues and that this phosphorylation inhibits TRAF2 interaction with the CD40 cytoplasmic domain (20, 21). However, TRAF2 phosphorylation sites and their functional significance in the TRAF2-CD40 interaction were not characterized in these studies.

We previously reported the identification of two phosphorylation sites (Ser-11 and Ser-55) in TRAF2 and showed that phosphorylation at these sites promotes the secondary but not the immediate phase of JNK and NF-κB activation following TNF-α stimulation (22, 23). However, the mechanisms by which TRAF2 phosphorylation regulates the secondary phase of the signaling pathways remain unknown. In the present study, we demonstrate that CD40 ligation induces TANK-binding kinase 1 (TBK1)-mediated TRAF2 phosphorylation on Ser-11 and that this phosphorylation leads to the dissociation of the effector complex from CD40 to the cytoplasm to initiate the secondary phase of canonical NF-κB activation. This Ser-11 phosphorylation and cytoplasmic translocation of the complex is not essential for initial JNK activation but is required for the full and prolonged activation of JNK. In the absence of Ser-11 phosphorylation, the TRAF2 RING domain binds directly to phospholipids and facilitates the translocation of TRAF2 and TRAF2-associated proteins to membrane lipid rafts, resulting in their degradation and subsequent activation of the noncanonical NF-κB

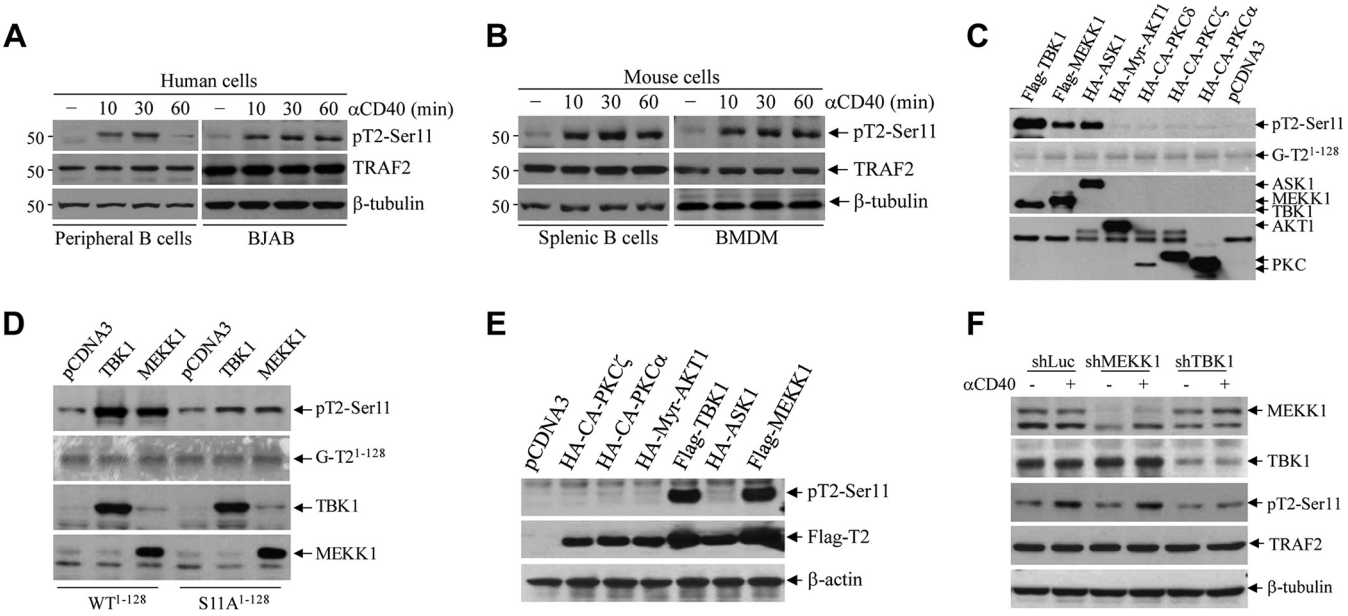

FIG 1 CD40 ligation elicits TBK1-mediated TRAF2 phosphorylation on Ser-11. (A and B) Human peripheral resting B cells ($CD19^+$ $CD43^-$) and BJAB B cell lymphoma cells (A) and mouse splenic B cells and bone marrow-derived macrophages (BMDMs) (B) were stimulated with anti-human CD40 (G28.5, 10 μg/ml) or anti-mouse CD40 (1C10, 5 μg/ml) agonistic antibodies (αCD40) for the indicated times. TRAF2 Ser-11 phosphorylation (pT2-Ser11) was then monitored by Western blotting with a site-specific phosphoantibody. (C) Kinases previously implicated in receptor-mediated NF-κB activation were expressed and immunopurified from 293T cells and then subjected to *in vitro* phosphorylation assays with GST-$TRAF2^{1-128}$ as the substrate. The reaction mixtures were separated by SDS-PAGE and transferred to nitrocellulose membrane, and TRAF2 phosphorylation was then assessed by autoradiography. The same membrane was stained with Ponceau S to visualize the substrate (GST-$TRAF2^{1-128}$) and then probed with anti-HA and anti-Flag antibodies to monitor the expression of kinases. (D) TBK1 and MEKK1 were immunopurified from 293T cells and subjected to *in vitro* phosphorylation assays using GST-TRAF2-WT^{1-128} and GST-TRAF2-$S11A^{1-128}$ as substrates as described in the legend to panel C. (E) 293T cells were cotransfected with TRAF2 and the indicated kinases, and 24 h after transfection, TRAF2 phosphorylation and expression of kinases were examined by Western blotting. (F) A20.2J TRAF2-WT cells stably transduced with shRNAs targeting MEKK1, TBK1, or firefly luciferase (Luc) were stimulated with 1C10 (αCD40; 5 μg/ml) for 30 min, and TRAF2 Ser-11 phosphorylation was monitored by Western blotting.

pathway. Collectively, these findings suggest that the primary function of the TRAF2 RING domain is to interact with phospholipids to control the fate of the CD40 signaling complex and that Ser-11 phosphorylation regulates such RING-phospholipid interactions to modulate spatiotemporal activation of the JNK and NF-κB pathways.

RESULTS

CD40 ligation elicits TRAF2 Ser-11 phosphorylation in hematopoietic cells. We previously identified two sites (Ser-11 and Ser-55) within the TRAF2 N terminus that are inducibly phosphorylated following TNF-α stimulation in MEFs and epithelial cancer cell lines (22, 23). To determine if CD40 ligation also induces TRAF2 phosphorylation in B cells and macrophages, we stimulated human peripheral resting B cells ($CD19^+$ $CD43^-$) and BJAB lymphoma cells with anti-human CD40 agonistic antibody (Ab) G28.5 (5 μg/ml) and mouse splenic $CD43^-$ B cells and bone marrow-derived macrophages (BMDMs) with anti-mouse CD40 agonistic Ab 1C10 (5 μg/ml). As shown by the results in Fig. 1A and B, CD40 ligation clearly elicited TRAF2 phosphorylation at Ser-11, starting by 10 min and peaking at 30 min poststimulation, and the kinetics of this phosphorylation was comparable to those previously described in MEFs and HeLa cells following TNF-α stimulation (22, 23). Notably, TRAF2 phosphorylation at Ser-55 was not clearly detected in mouse B cells and BMDMs in response to CD40 ligation (data not shown); therefore, we focused in the present study on the roles of TRAF2 Ser-11 phosphorylation in CD40 signaling.

TBK1 mediates CD40-induced TRAF2 Ser-11 phosphorylation. Several serine-threonine kinases have been implicated in TNFR superfamily-induced NF-κB and JNK activation, including TBK1 (also known as T2K), MEKK1, AKT, apoptosis signal-regulating kinase 1 (ASK1), receptor-interacting serine/threonine-protein kinase 1 (RIPK1), PKCα,

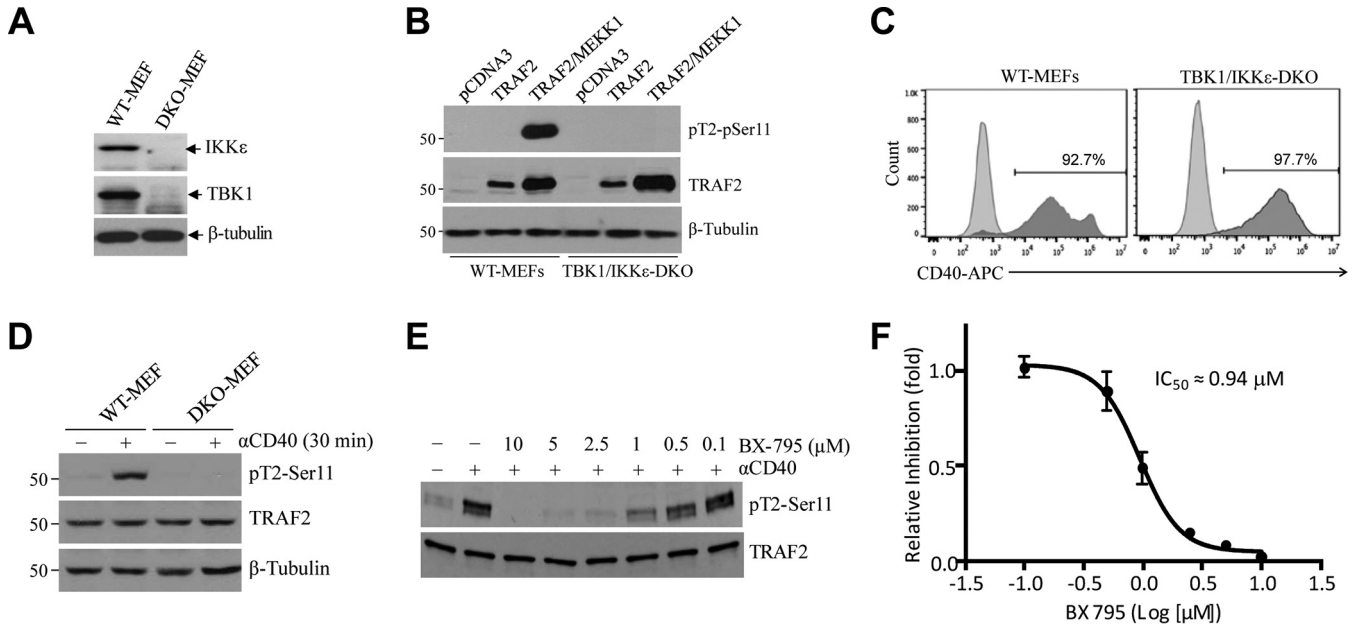

FIG 2 TBK1 directly phosphorylates TRAF2 at Ser-11. (A) Expression of TBK1 and IKKε in wild-type (WT) and TBK1/IKKε double-knockout (DKO) MEFs was analyzed by Western blotting. (B) TRAF2 Ser-11 phosphorylation was monitored in WT and TBK1/IKKε DKO MEFs following transient overexpression of TRAF2 with or without MEKK1. (C) WT and TBK1/IKKε DKO MEFs were stably transduced with pQCXIP-hCD40 (human CD40), and surface expression of hCD40 was then analyzed by FACS. (D) WT and TBK1/IKKε DKO MEFs stably expressing hCD40 were stimulated with G28.5 (αCD40; 10 μg/ml), and TRAF2 Ser-11 phosphorylation was examined by Western blotting. (E) A20.2J cells were pretreated with a TBK1 inhibitor (BX-795) as indicated before being stimulated with 1C10 (αCD40; 5 μg/ml) for 20 min, and then TRAF2 Ser-11 phosphorylation was monitored by Western blotting. (F) The TRAF2 Ser-11 phosphorylated-protein bands were quantified by densitometry, and the average levels of TRAF2 phosphorylation from three independent experiments were plotted in a log scale graph to measure dose response and 50% inhibitory concentration (IC_{50}) values. Data represent the mean values $\pm$ SD.

PKCε, and PKCζ (24–27). To test whether these kinases can phosphorylate TRAF2 on Ser-11, their wild-type (WT) or constitutively active (CA) forms (FLAG or hemagglutinin [HA] tagged) were transiently expressed in 293T cells, immunoprecipitated with anti-FLAG or -HA Abs, and then subjected to *in vitro* kinase assays using glutathione *S*-transferase (GST)-tagged N-terminal TRAF2 residues 1 to 128 (GST-TRAF2$^{1-128}$) as the substrate. As shown by the results in Fig. 1C, MEKK1 and TBK1 clearly phosphorylated GST-TRAF2$^{1-128}$ *in vitro*. To confirm that MEKK1 and TBK1 phosphorylate TRAF2 at Ser-11 *in vitro*, the same kinase assays were carried out using a GST-TRAF2 mutant with a mutation of Ser-11 to Ala (S11A) (GST-TRAF2-S11A$^{1-128}$) as the substrate, and the results demonstrated that MEKK1 and TBK1 fail to phosphorylate GST–TRAF2-S11A$^{1-128}$ *in vitro* (Fig. 1D). To further validate these findings, cotransfection experiments were performed in 293T cells with TRAF2 and the candidate kinases. As expected, a significant increase in TRAF2 Ser-11 phosphorylation was observed by Western blotting in the cells cotransfected with MEKK1 and TBK1 (Fig. 1E).

Next, to examine CD40-induced TRAF2 Ser-11 phosphorylation under more physiological conditions, small hairpin RNA (shRNA) vectors targeting mouse MEKK1 (shMEKK1), TBK1 (shTBK1), or firefly luciferase (shLuc) were stably expressed in A20.2J mouse B cells. Knockdown efficiencies of 70 to 90% were confirmed by Western blotting (Fig. 1F). Stimulation of these cells with 1C10 Ab (5 μg/ml) revealed that knockdown of TBK1, but not that of MEKK1, markedly decreased CD40-induced TRAF2 Ser-11 phosphorylation (Fig. 1F). To further clarify the potential roles of TBK1 and MEKK1 in TRAF2 Ser-11 phosphorylation in nontransformed cells, TBK1 and IKKε (encoded by a gene highly homologous to the TBK1 gene) double-knockout (DKO) and WT MEFs (Fig. 2A) were transiently transfected with TRAF2 with or without MEKK1. Western blotting revealed that cotransfection of MEKK1 markedly increased TRAF2 protein expression in both WT and TBK1/IKKε DKO MEFs, but a significant increase in TRAF2 Ser-11 phosphorylation was observed only in WT MEFs and not in DKO MEFs (Fig. 2B). To confirm these data, WT and TBK1/IKKε DKO MEFs were stably transfected

with human CD40 (WT-MEF-hCD40 and DKO-MEF-hCD40) (Fig. 2C) and monitored for TRAF2 Ser-11 phosphorylation following treatment with G28.5 (10 μg/ml). In line with the results in A20.2J-shTBK1 cells, TRAF2 Ser-11 phosphorylation was clearly detected only in WT-MEF-hCD40 cells and not in their DKO counterparts (Fig. 2D). Moreover, pretreatment of A20.2J cells with a TBK1-specific inhibitor (BX-795) also inhibited CD40-induced TRAF2 Ser-11 phosphorylation in a dose-dependent manner, with a 50% inhibitory concentration (IC_{50}) of 0.94 μM (Fig. 2E and F). These results are in line with a previous report that IKKε phosphorylates TRAF2 at Ser-11 in breast cancer cells (28). Of note, amino acids surrounding the Ser-11 residue (N-PG^{11}SL-C) form a consensus phosphorylation motif for TBK1 and IKKε but not for MEKK1 or AKT1 (28). Collectively, these data suggest that TBK1, but not MEKK1, directly phosphorylates TRAF2 at Ser-11 in response to CD40 ligation.

TRAF2 Ser-11 phosphorylation is required for CD40-induced full activation of JNK and the secondary phase of NF-κB activation. To assess the roles of TRAF2 Ser-11 phosphorylation in CD40 signaling, we attempted to stably express TRAF2-WT and -S11A in A20.2J-TRAF2-KO cells (A20-TRAF2-WT and -S11A) at a physiological level through serial dilution of retroviral supernatants. However, in several independent experiments, we found that the protein expression of TRAF2-S11A was always lower than that of TRAF2-WT, especially when high-titer retroviral supernatants were used for infection (Fig. 3A). Treatment of A20-TRAF2-WT and -S11A cells with a proteasome inhibitor (MG132) or a lysosomal inhibitor (chloroquine) revealed that overexpressed TRAF2-S11A is constantly degraded through a lysosomal pathway under unstimulated conditions (Fig. 3B). Nevertheless, 3-fold dilutions of retroviral supernatants gave rise to similar amounts of TRAF2-WT and -S11A protein expression at a physiological level, albeit TRAF2-S11A expression was still slightly lower than that of TRAF2-WT (Fig. 3A, 3-fold-dilution lanes). Therefore, for the subsequent functional assays, we used stable cell lines generated with 3-fold-diluted retroviral supernatants. As expected, TRAF2 Ser-11 phosphorylation occurred only in A20-TRAF2-WT cells, with kinetics similar to those observed in primary B cells (Fig. 3C). Since cytokines induce two phases (early and secondary) of JNK and IKK activation in most cell types (29–31), we stimulated A20-TRAF2-WT and -S11A cells with 1C10 and monitored the kinetics of JNK and NF-κB pathway activation over a period of 3 h (Fig. 3D). Interestingly, both the early (10 to 30 min) and secondary (120 to 180 min) phases of JNK activation were clearly dampened in A20-TRAF2-S11A cells compared to the results in A20-TRAF2-WT counterparts. With respect to the NF-κB pathway, A20-TRAF2-WT cells exhibited biphasic IKK activation with peaks at 10 and 60 min after CD40 ligation. However, in A20-TRAF2-S11A cells, the early phase was activated normally but the secondary phase was entirely absent. In line with these results, p65 phosphorylation was also dampened in A20-TRAF2-S11A cells. The results of three experiments from three independently established cell lines were quantified by densitometry, and the differences in JNK and IKK activation kinetics were determined to be statistically significant (Fig. 3E). On the other hand, cIAP1 degradation was slightly faster in A20-TRAF2-S11A cells, whereas TRAF3 degradation was comparable between A20-TRAF2-WT and -S11A cells. These data indicate that TRAF2 Ser-11 phosphorylation is required for the full and prolonged activation of IKK and JNK following CD40 ligation.

TRAF2 Ser-11 phosphorylation is required for the expression of a subset of NF-κB target genes. The NF-κB family of transcription factors is capable of inducing the expression of hundreds of genes, and their transcriptional specificity and temporal dynamics are controlled by several regulatory modules, including but not limited to accessory molecules, relative levels of abundance of different NF-κB subunits and heterodimerization, affinity differences among NF-κB heterodimers for different κB sites, promoter accessibility, and the chromatin microenvironment (24, 32). To determine the effect of the secondary phase of the NF-κB pathway on target gene expression, we stimulated A20-TRAF2-WT and -S11A cells with 1C10, as well as with pretrimerized MegaCD40L, which mimics membrane-bound CD40L (33), and then assessed the expression of NF-κB target genes by real-time quantitative reverse transcription-PCR

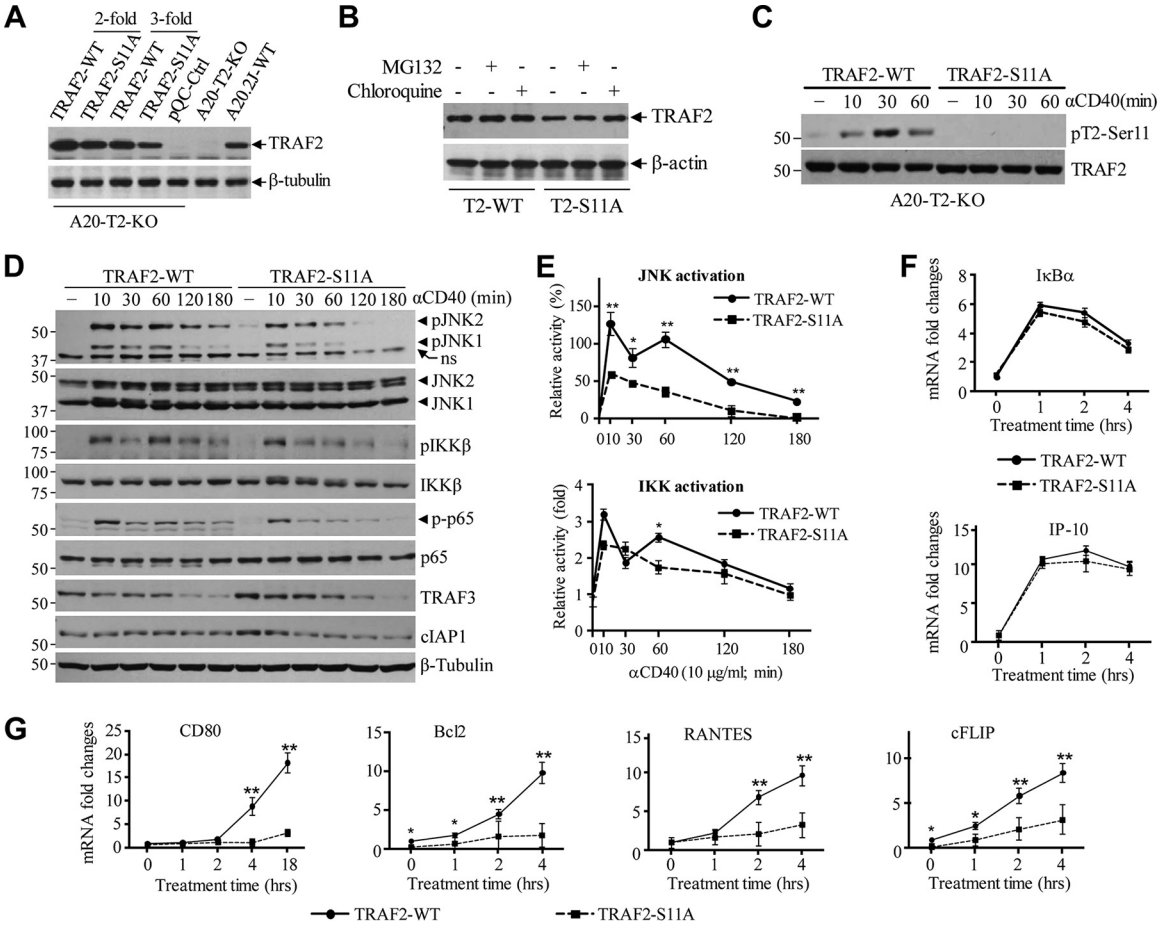

FIG 3 TRAF2 Ser-11 phosphorylation regulates full activation of JNK and the secondary phase of the canonical NF-κB pathway following CD40 ligation. (A) Retroviral supernatants of pBabe-TRAF2-WT and -S11A were diluted 2- and 3-fold before being used for infection of A20.2J-TRAF2-KO (A20-T2-KO) cells. After puromycin selection, exogenous TRAF2 expression in A20-TRAF2-WT and -S11A cells was analyzed in parallel with that of endogenous TRAF2 in parental A20.2J-WT cells by Western blotting. (B) A20-T2-KO cells reconstituted with TRAF2-WT or -S11A were treated with proteasome inhibitor MG132 (20 μM) or lysosome inhibitor chloroquine (100 μM) for 6 h, and then TRAF2 expression was monitored by Western blotting. (C) A20-TRAF2-WT and -S11A cells were stimulated with 1C10 (5 μg/ml) as indicated, and TRAF2 Ser-11 phosphorylation was examined by Western blotting. (D and E) A20-TRAF2-WT or -S11A cells were treated with 1C10 (5 μg/ml) as indicated, and phosphorylation of JNK, IKK, and p65, as well as the degradation of TRAF3 and cIAP1, were examined by Western blotting; JNK and IKK phosphorylation from three independent experiments was then quantified by densitometry, and the results (mean values ± SD) were plotted in the graphs. *, $P < 0.05$; **, $P < 0.01$. (F and G) A20-TRAF2-WT or -S11A cells were stimulated with MegaCD40L, and the expression of indicated gene products was analyzed by quantitative RT-PCR. Data represent the mean values ± SD from three independent experiments. *, $P < 0.05$; **, $P < 0.01$.

(qRT-PCR). Both types of stimulation gave rise to a similar gene expression profile, with MegaCD40L inducing more robust gene expression (Fig. 3F and G and data not shown). Interestingly, TRAF2 Ser-11 phosphorylation had no substantial effect on the induction of IκBα (*Nfkiba*) or IP-10 (*Cxcl10*); however, the levels of upregulation of RANTES (*Ccl5*) and CD80 (*Cd80*) were significantly dampened in A20-TRAF2-S11A cells compared to the levels in A20-TRAF2-WT cells. Furthermore, the expression levels of the prosurvival Bcl2 (*Bcl2*) and cFLIP (*Cflar*) genes were also considerably lower both before and after CD40 ligation in A20-TRAF2-S11A cells. Therefore, these data suggest that CD40-induced TRAF2 Ser-11 phosphorylation is required for the efficient induction of a subset of NF-κB target genes.

TRAF2 Ser-11 phosphorylation regulates the translocation of the signaling complex from CD40 to the cytoplasm. To determine the possible mechanisms underlying TRAF2 Ser-11 phosphorylation-dependent full activation of JNK and IKK following CD40 ligation, we sought to examine the subcellular localization of effector proteins. First, we prepared fractions that were soluble and insoluble in nonionic

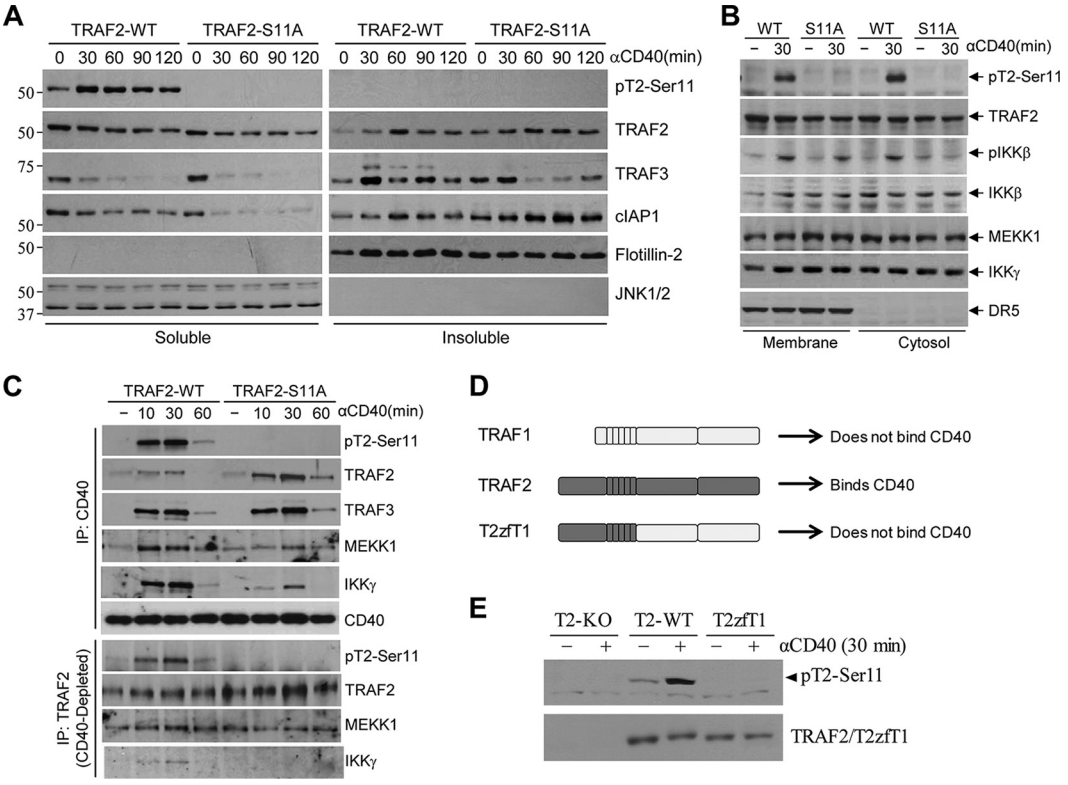

FIG 4 TRAF2 Ser-11 phosphorylation regulates the cytoplasmic translocation of the signaling complex. (A) Nonionic detergent soluble and insoluble fractions were prepared from A20-TRAF2-WT or -S11A cells treated with 1C10 (5 μg/ml) as indicated, and the localization of phosphorylated and nonphosphorylated TRAF2, TRAF3, and cIAP1 in these fractions was monitored by Western blotting. (B) Membrane and cytosolic fractions were isolated from A20-TRAF2-WT and -S11A cells following CD40 stimulation, and the localization of indicated phosphorylated and nonphosphorylated proteins was monitored by Western blotting. (C) A20-TRAF2-WT and -S11A cells were treated with 1C10 (5 μg/ml) as indicated, and the CD40-associated membrane complex was immunoprecipitated first; after that, the TRAF2-associated cytosolic complex was immunoprecipitated from the CD40-depleted lysates. Recruitment of the indicated proteins to the complexes was then assessed by Western blotting. (D) A diagram showing schematically the domains of TRAF1, TRAF2, and TRAF1-TRAF2 fusion (T2zfT1) proteins. (E) A20-T2-KO cells reconstituted with TRAF2-WT or T2zfT1 were treated with 1C10 (5 μg/ml) as indicated, and TRAF2 phosphorylation was then monitored by Western blotting.

detergent (e.g., 0.5% Triton X-100) from A20-TRAF2-WT and -S11A cells before and after CD40 ligation. As shown by the results in Fig. 4A, the steady-state levels of TRAF2 and cIAP1 proteins were markedly higher in the insoluble fraction of A20-TRAF2-S11A cells than in that of A20-TRAF2-WT cells before stimulation. Following stimulation, more cIAP1 and less TRAF3 had accumulated in the insoluble fraction of A20-TRAF2-S11A cells. Next, we prepared membrane and cytoplasmic fractions from A20-TRAF2-WT and -S11A cells by homogenizing the cell pellets in detergent-free hypotonic buffer and then assessed the localization of effector proteins. Interestingly, similar to the accumulation of TRAF2 and cIAP1 in the insoluble fractions in A20-TRAF2-S11A cells, both MEKK1 and IKKγ were evident in the membrane fraction of unstimulated A20-TRAF2-S11A cells, and stimulation with 1C10 did not further increase their protein levels in this fraction. Conversely, in A20-TRAF2-WT cells, 1C10 stimulation resulted in the recruitment of MEKK1 and IKKγ to the membrane fractions (Fig. 4B). To confirm these results, we performed coimmunoprecipitation assays to evaluate the components of the CD40 and TRAF2 signaling complex. Total cell lysates were prepared, and the CD40 receptor complex was first immunoprecipitated with 1C10. Then, the CD40 complex-depleted lysates were subjected to immunoprecipitation with anti-TRAF2 Ab. As expected, the recruitment of TRAF2 and TRAF3 to CD40 was not affected by TRAF2 Ser-11 phosphorylation (Fig. 4C). However, in A20-TRAF2-S11A cells, even though relatively more TRAF2-S11A was found in the CD40 complex, the recruitment of MEKK1 and IKKγ to the CD40 complex was clearly reduced compared to their recruitment in A20-TRAF2-WT

cells. Presumably, TRAF2 protein expression is severalfold higher than the expression of MEKK1 and IKKγ in A20.2J cells; as such, significant portions of MEKK1 and IKKγ may be associated with TRAF2-S11A in the membrane fractions, limiting the availability of MEKK1 and IKKγ proteins in the cytoplasm of TRAF2-S11A cells. Nevertheless, consistent with the previous findings by Matsuzawa et al. (14), coimmunoprecipitation of TRAF2 from CD40 complex-depleted lysate revealed that TRAF2 formed a complex with MEKK1 and IKKγ in the cytoplasm of A20-TRAF2-WT cells following CD40 ligation (Fig. 4C). However, this cytoplasmic complex was totally absent in A20-TRAF2-S11A cells. This led us to the hypothesis that TRAF2 Ser-11 phosphorylation occurs within the CD40 complex and that this phosphorylation regulates the translocation of the signaling complex from CD40 to the cytoplasm. Given that TRAF1 does not directly bind to CD40 (34), to test our hypothesis, we generated a TRAF2-TRAF1 chimeric molecule, consisting of the TRAF2 N terminus and TRAF1 C terminus (T2zfT1) (Fig. 4D), and stably expressed it in A20-TRAF2-KO cells. As expected, CD40 ligation induced TRAF2 Ser-11 phosphorylation in A20-TRAF2-WT cells but not in A20-T2zfT1 cells (Fig. 4E), suggesting that TRAF2 Ser-11 phosphorylation occurs within the CD40 complex but not in the cytoplasm. Collectively, these data suggest that (i) TRAF2 Ser-11 phosphorylation is required for the translocation of the signaling complex from CD40 to the cytoplasm, which is essential for the full activation of JNK and IKK, and (ii) in the absence of TRAF2 Ser-11 phosphorylation, the signaling complex remains in the membrane fraction and then translocates to lipid rafts, where it is eventually internalized and degraded by the lysosome.

TRAF2 Ser-11 phosphorylation inhibits CD40-mediated noncanonical NF-κB activation. CD40 ligation activates both the canonical and noncanonical NF-κB pathways. To test the effect of TRAF2 Ser-11 phosphorylation on the noncanonical NF-κB pathway, we attempted to analyze the processing of p100 to p52 in parental A20.2J and A20-TRAF2-KO cells following CD40 ligation. However, the full-length p100 protein was not detected in A20.2J cells by Western blotting, while it was clearly detected under the same conditions in TRAF2-KO CH12.LX (CH12-T2-KO) and BJAB B cell lines (Fig. 5A). It appears that in A20.2J cells, either the p100 protein is constitutively processed to p52 or the gene is mutated or deleted at the C-terminal region. Thus, we transitioned into CH12-T2-KO cells to assess the roles of TRAF2 Ser-11 phosphorylation in noncanonical NF-κB pathway activation (35). For this, CH12-T2-KO cells were reconstituted with TRAF2-WT or -S11A (CH12-T2-WT and -S11A) with the same methods used to generate the A20.2J lines. Interestingly, TRAF2 protein expression levels were also lower in CH12-T2-S11A cells than in CH12-T2-WT cells, even with 3-, 4- and 5-fold dilutions of retroviral supernatants for the infection (Fig. 5B and data not shown). Quantitative and semiquantitative RT-PCR analyses revealed that the gene expression levels at the mRNA level were similar in CH12-T2-WT and -S11A cells (Fig. 5C and D). Similar to A20-T2-S11A cells, chloroquine treatment, but not MG132 treatment, stabilized TRAF2-S11A protein, suggesting that TRAF2-S11A was constantly degraded through the lysosomal pathway in CH12-T2-S11A cells (Fig. 5E). Nevertheless, CD40 ligation induced TRAF2 Ser-11 phosphorylation in CH12-T2-WT cells but not in CH12-T2-S11A cells, with kinetics similar to those observed in A20.2J cells (Fig. 5F). As expected, CD40 stimulation triggered the processing of p100 to p52 in CH12-T2-WT cells, whereas in CH12-T2-S11A cells, p100 was constitutively processed to p52 to a great extent without CD40 ligation (Fig. 5G). In addition, the steady-state level of endogenous cIAP1 protein was also clearly reduced in CH12-T2-S11A cells compared to the level in CH12-T2-WT cells. In line with this, the kinetics of TRAF3 degradation were delayed in CH12-T2-S11A cells. It seems that cIAP1 expression is considerably lower in CH12.LX cells than in A20.2J cells; as such, a significant portion of cIAP1 protein is degraded in CH12-TRAF2-S11A cells compared to that in A20-TRAF2-S11A cells, which explains why TRAF3 degradation is delayed in CH12-TRAF2-S11A cells following CD40 ligation.

To further examine the roles of TRAF2 Ser-11 phosphorylation in p100 processing, we stimulated WT-MEF-hCD40 and DKO-MEF-hCD40 cells with anti-human CD40 MAb (G28.5) and examined p100 processing. As shown by the results in Fig. 5H, CD40

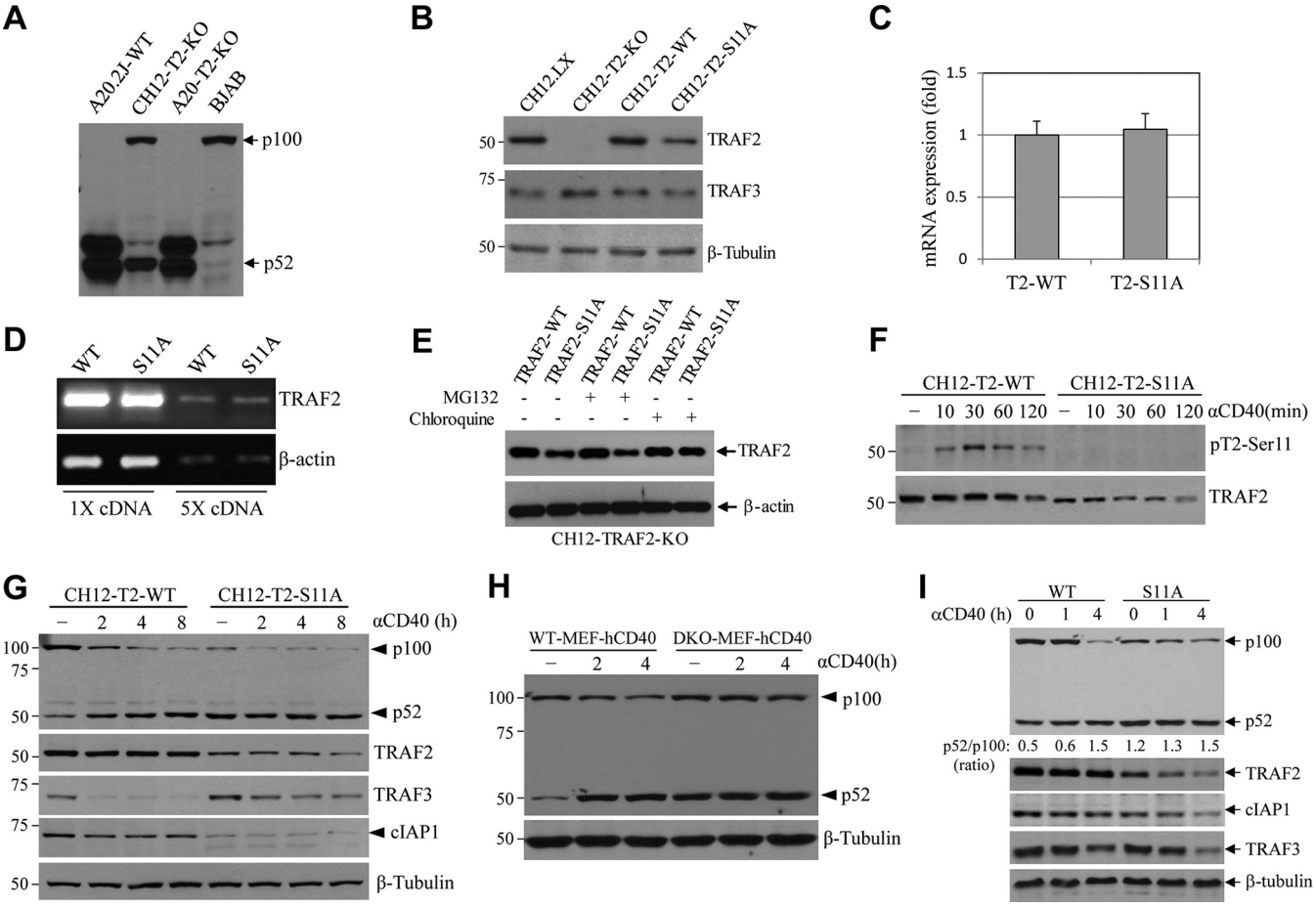

FIG 5 TRAF2 Ser-11 phosphorylation inhibits noncanonical NF-κB activation. (A) Expression of p100 and p52 in indicated cells was monitored by Western blotting. (B) Basal TRAF2 and TRAF3 expression in CH12-T2-KO cells reconstituted with TRAF2-WT or -S11A was examined by Western blotting, in parallel with their expression in parental CH12.LX and CH12-T2-KO cells. (C and D) Exogenous TRAF2 mRNA expression in CH12-T2-WT and -S11A cells was examined by real-time and conventional RT-PCR. Data in panel C represent the mean values ± SD. (E) CH12-T2-WT and -S11A cells were treated with MG132 (20 μM) or chloroquine (100 μM) for 6 h, and then TRAF2 expression was monitored by Western blotting. (F and G) CH12-T2-WT or -S11A cells were treated with 1C10 (5 μg/ml) as indicated, and TRAF2 phosphorylation, p100 processing to p52, and degradation of TRAF2, TRAF3, and cIAP1/2 were assessed by Western blotting. (H) p100 processing to p52 in WT and TBK1/IKKε DKO MEFs stably expressing hCD40 was monitored by Western blotting. (I) WT MEFs expressing hCD40 were stably transduced with TRAF2-WT and -S11A, and basal and CD40-induced p100 processing to p52 and degradation of TRAF2, TRAF3, and cIAP1 were examined by Western blotting.

ligation induced the processing of p100 to p52 in WT-MEF-hCD40 cells; however, in DKO-MEF-hCD40 cells, p100 was constitutively processed to p52 to a great extent before CD40 ligation. Next, we stably overexpressed TRAF2-WT or -S11A in WT-MEF-hCD40 cells (WT-MEF-hCD40-TRAF2-WT and -S11A) and examined p100 processing. Consistently, CD40 ligation induced p100 processing in WT-MEF-hCD40-TRAF2-WT cells, whereas in WT-MEF-hCD40-TRAF2-S11A cells, p100 was constitutively processed to p52 before stimulation and endogenous cIAP1 protein was significantly reduced (Fig. 5I). Collectively, these data suggest that TBK1-mediated TRAF2 Ser-11 phosphorylation inhibits noncanonical NF-κB activation by preventing TRAF2-cIAP1 complex translocation to lipid rafts and the subsequent degradation.

TRAF2 Ser-11 phosphorylation also regulates CD40- and TNF-α-induced full activation of JNK and the secondary phase of NF-κB activation in human cells. To further characterize the roles of TRAF2 Ser-11 phosphorylation in JNK and NF-κB activation in response to CD40 and TNFR1 ligations in human cells, we reconstituted TRAF2-deficient human HAP1 (HAP1-T2-KO) cells with TRAF2-WT or -S11A (HAP1-T2-WT or -S11A) with the same methods used to generate the A20-T2-KO and CH12-T2-KO lines. As expected, TRAF2 protein expression levels were lower in HAP1-T2-S11A cells than in the corresponding HAP1-T2-WT cells (Fig. 6A). Stimulation of these cells with

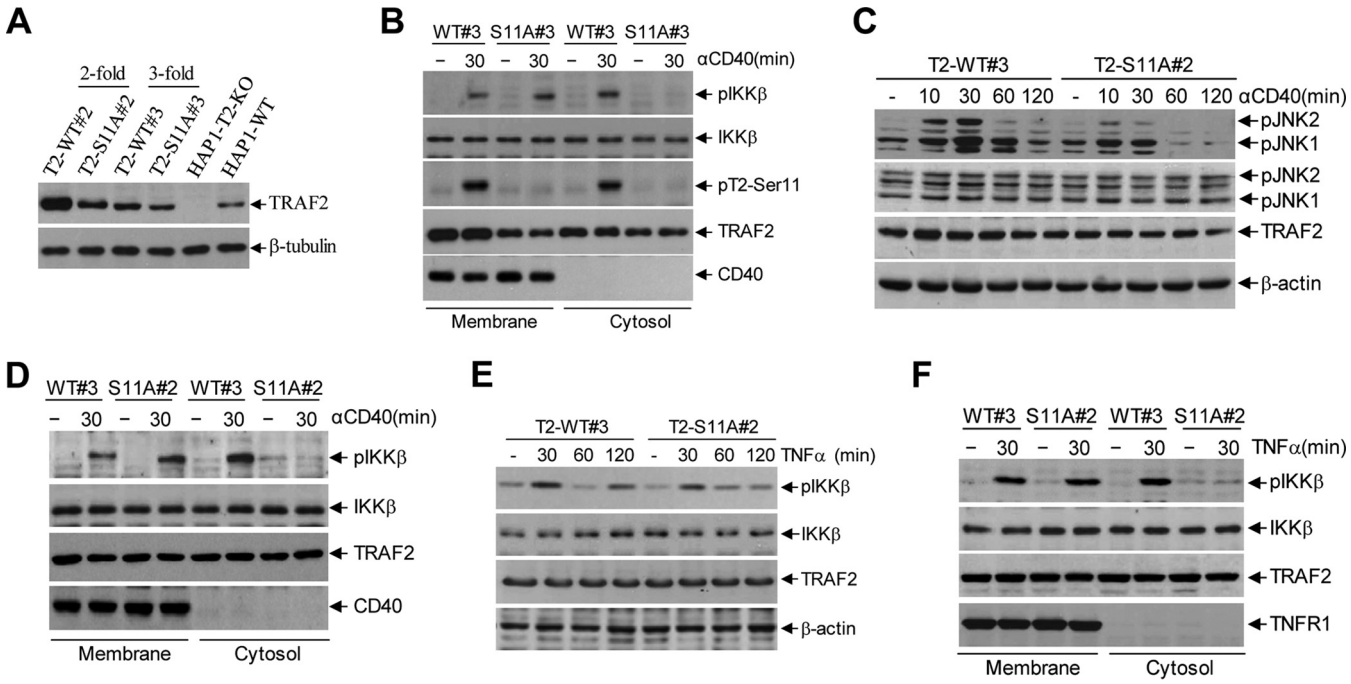

FIG 6 TRAF2 Ser-11 phosphorylation regulates full activation of JNK and the secondary phase of the canonical NF-κB pathway in human cells following CD40 and TNFR1 ligation. (A) Retroviral supernatants of pBabe-TRAF2-WT and -S11A were diluted 2- and 3-fold before being used for infection of human HAP1-T2-KO cells. After puromycin selection, exogenous TRAF2 expression was analyzed in parallel with endogenous TRAF2 expression in parental cells by Western blotting. (B) Membrane and cytosolic fractions were isolated from HAP1-T2-WT#3 and -S11A#3 cells following G28.5 (10 μg/ml) stimulation, and the localization of indicated phosphorylated and nonphosphorylated proteins was monitored by Western blotting. (C) HAP1-T2-WT#3 and -S11A#2 cells were treated with G28.5 (10 μg/ml), and phosphorylation of JNK was examined by Western blotting. (D) Membrane and cytosolic fractions were isolated from HAP1-T2-WT#3 and -S11A#2 cells following CD40 ligation with G28.5 (10 μg/ml), and the localization of indicated phosphorylated and nonphosphorylated proteins was monitored by Western blotting. (E) HAP1-T2-WT#3 and -S11A#2 cells were treated with TNF-α (20 ng/ml), and phosphorylation of IKK was examined by Western blotting. (F) Membrane and cytosolic fractions were isolated from HAP1-T2-WT#3 and -S11A#2 cells following TNF-α (20 ng/ml) stimulation, and the localization of indicated phosphorylated and nonphosphorylated proteins was monitored by Western blotting.

G28.5 (10 μg/ml) revealed that phospho-IKKβ was detectable only in the cytoplasm of HAP1-T2-WT cells and not in HAP1-T2-S11A cells (Fig. 6B), suggesting that the signaling complex was unable to translocate to the cytoplasm in human cells in the absence of TRAF2 Ser-11 phosphorylation. Notably, HAP1-T2-S11A#2 cells reconstituted with 2-fold-diluted retroviral supernatant expressed TRAF2 protein at a level comparable to that in HAP1-T2-WT#3 cells reconstituted with 3-fold-diluted retroviral supernatant. Analyses of JNK and NF-κB pathway activation in these cells revealed that CD40-induced JNK activation was dampened and phospho-IKK was absent in the cytoplasm of TRAF2-S11A#2 cells as well (Fig. 6C and D), confirming that the reduced activation of JNK and the secondary phase of NF-κB activation in TRAF2-S11A cells is not due to inefficient expression of TRAF2-S11A protein. Stimulation of HAP1-T2-WT#3 and -S11A#2 cells with TNF-α and subsequent analyses of IKKβ phosphorylation revealed that the secondary phase of IKK phosphorylation was impaired and phospho-IKK was absent in the cytoplasm of T2-S11A#2 cells (Fig. 6E and F), suggesting that the two-stage signaling mechanism also applies to other TNF family members.

TRAF2 Ser-11 phosphorylation inhibits TRAF2 RING-dependent translocation to the multivesicular bodies. In TRAF2 phosphorylation studies, we consistently noticed differential expression and localization of N- and C-terminally FLAG-tagged TRAF2-S11A (nFLAG-TRAF2-S11A and TRAF2-S11A-cFLAG) in HeLa cells and MEFs (unpublished data). To further understand the possible mechanisms for TRAF2 Ser-11 phosphorylation-dependent regulation of TRAF2 localization in the cells, we generated several mutant forms of TRAF2 (Fig. 7A) and transiently transduced them into HeLa cells to examine their subcellular localization by immunofluorescence (IF) staining. As expected, nFLAG-TRAF2-WT and TRAF2-WT-cFLAG displayed diffuse cytoplasmic localiza-

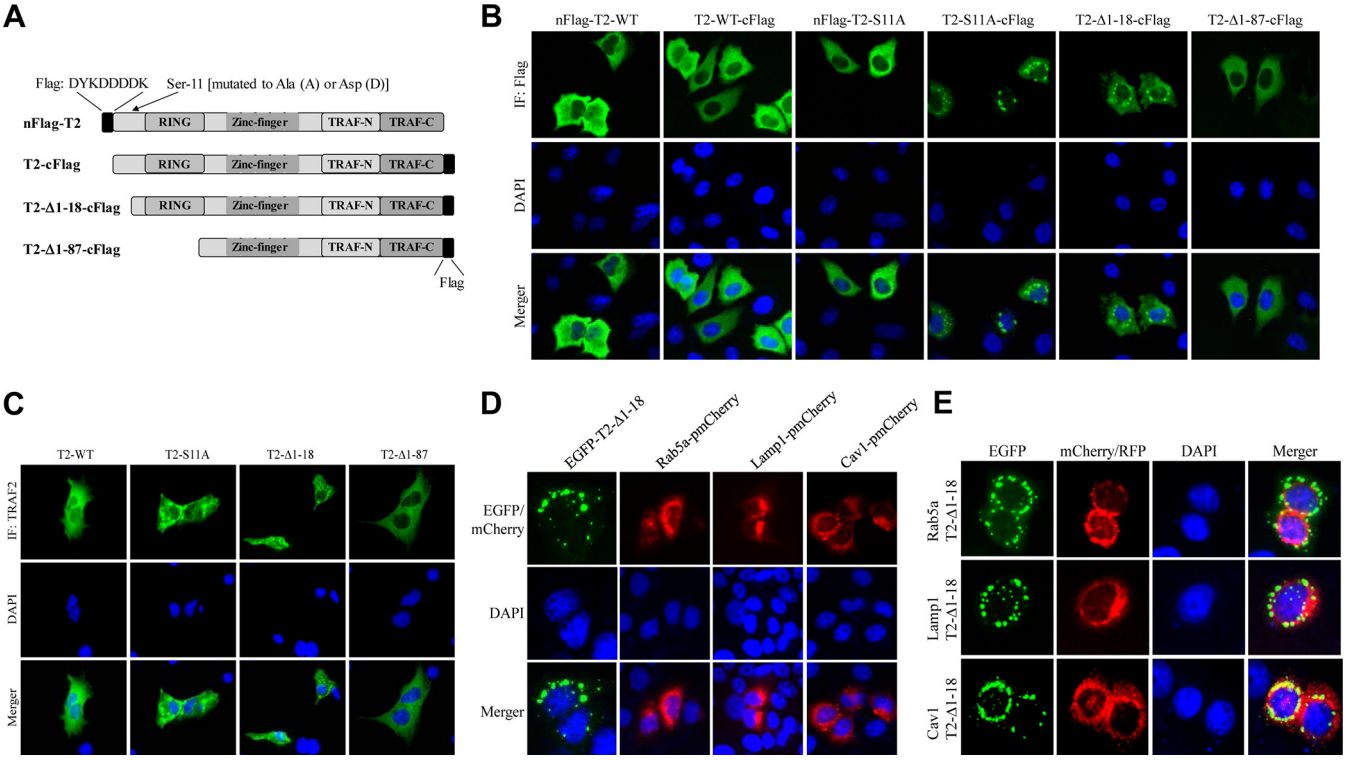

FIG 7 TRAF2 Ser-11 phosphorylation regulates its subcellular localization. (A) A diagram showing schematically the full-length and truncated forms of TRAF2 constructs, as well as their N- or C-terminal Flag tags. (B) HeLa cells cultured on glass coverslips were transfected with the indicated Flag-tagged TRAF2 plasmids, and 36 h after transfection, the cells were stained with fluorescein isothiocyanate (FITC)-labeled anti-FLAG antibody and DAPI to visualize TRAF2 localization and nuclei under an immunofluorescence (IF) microscope. (C) TRAF2/5 DKO MEFs cultured on glass coverslips were transfected with the indicated nontagged TRAF2 plasmids, and 36 h after transfection, the cells were stained with anti-TRAF2 antibody and DAPI to visualize TRAF2 localization. (D) HeLa cells cultured on glass coverslips were transfected with the indicated plasmids, and 36 h after transfection, the cells were fixed and stained with DAPI. The localization of corresponding proteins was then visualized by IF microscope. (E) EGFP-TRAF2-Δ1-18 was cotransfected with Rab5a-pmCherryC1, Lamp1-RFP, or Cav1-mRFP to HeLa cells, and their localizations in the cells were observed under IF microscope.

tion, as did nFLAG-TRAF2-S11A; however, TRAF2-S11A-cFLAG localized to the perinuclear punctate structures known as multivesicular bodies (MVBs) (Fig. 7B). A TRAF2 mutant with the N-terminal 18 amino acids deleted (TRAF2-Δ1-18-cFLAG) also localized to MVBs, while further deletion of the RING domain (TRAF2-Δ1-87-cFLAG) prevented MVB localization. Next, we transiently expressed nontagged TRAF2 mutants in TRAF2/5 DKO MEFs for IF staining with anti-TRAF2 C terminus Ab. As shown by the results in Fig. 7C, TRAF2-WT and TRAF2-Δ1-87 exhibited diffuse cytoplasmic expression, whereas TRAF2-S11A and TRAF2-Δ1-18 localized to MVBs. To further characterize the localization of TRAF2-S11A, we used enhanced green fluorescent protein by subcloning TRAF2-Δ1-18 into pCDNA3-EGFP (EGFP-T2-Δ1-18) and transfecting the plasmid into HeLa cells. Interestingly, EGFP-T2-Δ1-18 localized almost entirely to the perinuclear punctate structure (Fig. 7D). Cotransfection into HeLa cells of EGFP-T2-Δ1-18 and one of three proteins tagged with red fluorescent protein (RFP), namely, Rab5a-pmCherry (an early endosome marker), Lamp1-RFP (a lysosome marker), or Cav1-mRFP (a marker of lipid rafts and caveosomes [caveola-mediated endocytic vesicles]), revealed that TRAF2-Δ1-18 largely colocalizes with caveolin-1 (Cav1) to the perinuclear caveosomes (Fig. 7E). In separate experiments in 293T cells, Western blot and RT-PCR analyses revealed that the protein expression level of TRAF2-S11A-cFLAG was clearly lower than those of nFlag-TRAF2-WT, nFlag-TRAF2-S11A, and TRAF2-WT-cFlag, while their mRNA expression levels were comparable (Fig. 8A). Sucrose gradient isolation of lipid rafts revealed that significantly more TRAF2-S11A-cFLAG than TRAF2-WT-cFLAG accumulated in lipid rafts (Fig. 8B). These data suggest that TRAF2 Ser-11 phosphorylation inhibits TRAF2 RING-dependent localization to lipid rafts and subsequent caveola-mediated endocytosis to caveosomes and that the N-terminal Flag tag (DYKDDDDK), which contains five nega-

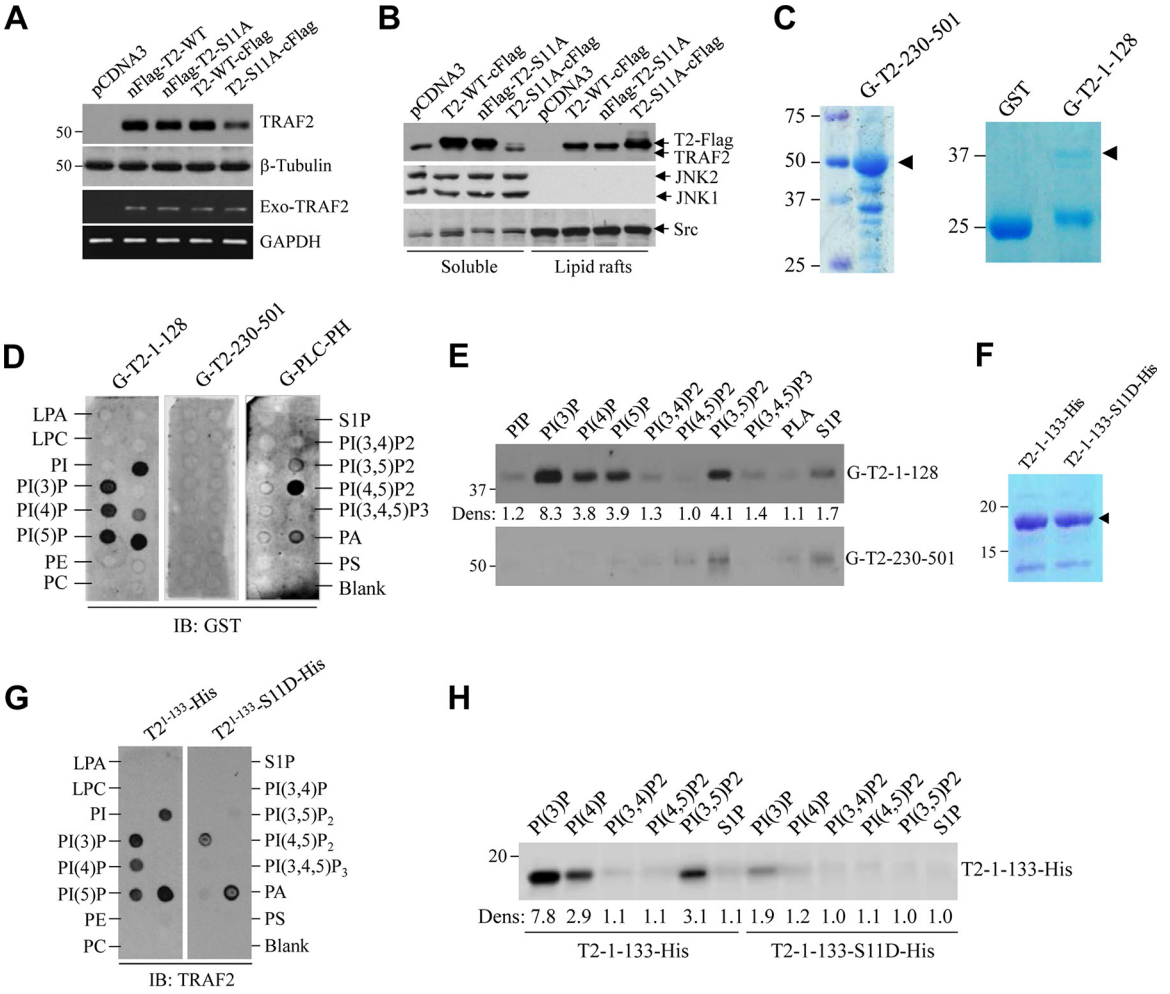

FIG 8 TRAF2 Ser-11 phosphorylation regulates its phospholipid binding. (A) The indicated TRAF2 constructs with N- or C-terminal Flag tags were transiently expressed in 293T cells, and 36 h after transfection, exogenous TRAF2 protein and mRNA expression were monitored by Western blotting and RT-PCR. (B) The indicated TRAF2 constructs were transiently expressed in 293T cells, and the presence of TRAF2 in the soluble and lipid raft fractions was monitored by Western blotting. (C) GST-tagged TRAF2 N-terminal (G-T2-1-128) and C-terminal (G-T2-230-501) domains were expressed in BL21 *E. coli* cells and purified with glutathione (GSH) beads. (D) Phospholipid binding abilities of G-T2-1-128 and G-T2-230-501 were examined by lipid-protein overlay assays using purified proteins and membrane-immobilized phospholipids, with G-PLC-PH as a control for PI(4,5)P binding. (E) Purified G-T2-1-128 and G-T2-230-501were incubated with various lipid affinity matrices for 60 min at 4°C; after that, the beads were washed extensively, and protein-lipid binding was assessed by Western blotting using anti-GST Ab. The intensities of bands were quantified by densitometry; the weakest band [PI(4,5)P2] was set as 1.0, and the rest were normalized to the PI(4,5)P2 signal. (F) C-terminally His-tagged TRAF2-1-133 (T2-1-133-His) and T2-1-133-S11D-His were expressed in BL21 *E. coli* cells and purified with Ni-NTA beads. (G) Phospholipid binding abilities of T2-1-133-His and T2-1-133-S11D-His were examined as described in the legend to panel D, using anti-TRAF2 Ab. (H) Purified T2-1-133-His and T2-1-133-S11D-His were incubated with indicated lipid affinity matrices for 60 min at 4°C, and then the beads were washed extensively before being assessed for protein-lipid binding by Western blotting. The intensities of bands were quantified as described in the legend to panel E.

tively charged Asp (D) residues, functionally mimics TRAF2 Ser-11 phosphorylation and interferes with TRAF2 RING domain-mediated translocation to lipid rafts.

TRAF2 Ser-11 phosphorylation regulates its RING-dependent phospholipid binding ability. The FYVE zinc finger is structurally similar to the RING and PHD domains, and FYVE domain-containing proteins (e.g., EEA1) interact with phospholipids (e.g., phosphatidylinositol-3-phosphate [PI3P]) to regulate vacuolar protein sorting and endosome function (36). Alvarez et al. previously reported that sphingosine-1-phosphate (S1P) binds the TRAF2 RING domain to promote its E3 ligase activity (5). These findings and our data led us to examine the possible interaction between the TRAF2 RING domain and phospholipids and the effect of TRAF2 Ser-11 phosphorylation on this interaction. To do so, we first attempted to express and purify a His-tagged protein comprising TRAF2 amino acids 1 to 87 (His-TRAF2-1-87) from *Escherichia coli*,

but the solubility of this protein was very poor even in the presence of 0.5% Triton X-100, and it was difficult to elute from Ni-nitrilotriacetic acid (NTA) beads. In contrast, the solubility of GST-TRAF2-1-128 in *E. coli* was much better in buffers containing 0.25% Triton X-100 (Fig. 8C), and yet, both His-TRAF2-1-87 and GST-TRAF2-1-128 precipitated when the detergent was removed. On the other hand, the bacterially expressed and purified TRAF2 C-terminal domain (GST-TRAF2-230-501) was still soluble when the detergent was removed. We carried out protein-lipid overlay assays in the presence of 0.25% Triton X-100, which revealed that purified GST-TRAF2-1-128 binds PI3P, PI4P, PI5P, PI(3,5)P2, and phosphatidic acid (PA) but not S1P (Fig. 8D). On the other hand, lipid affinity matrix pulldown assays revealed that GST-TRAF2-1-128 interacts strongly with PI3P, PI4P, PI5P, and PI(3,5)P2 and weakly with S1P (Fig. 8E). These data suggest that either the TRAF2 RING domain is very sticky and binds several different phospholipids or the N-terminal GST tag interferes with the binding specificity of the TRAF2 RING domain. Thus, to further define the interactions between the TRAF2 RING domain and phospholipids, we expressed and purified C-terminally His-tagged TRAF2-1-133-His from *E. coli* (Fig. 8F). Although the solubility of TRAF2-1-133-His was better than that of GST-TRAF2-1-128 in 0.25% Triton X-100, it still precipitated when the detergent was removed. Protein-lipid overlay and lipid affinity matrix pulldown assays revealed that the phospholipid binding ability of TRAF2-1-133-His was largely similar to that of GST-TRAF2-1-128, with the exception that TRAF2-1-133-His bound strongly to PI3P and poorly or not at all to S1P (Fig. 8G and H). Mutation of Ser-11 to phosphomimetic Asp (D) inhibited the phospholipid binding ability of TRAF2-1-133-His significantly but not completely. Notably, liposome-based assays are superior to protein-lipid overlay assays when it comes to measuring the binding affinities of proteins to phospholipids (37); however, the precipitation of GST-TRAF2-1-128 and TRAF2-1-133-His in detergent-free buffers prevented us from using this approach. Collectively, these data suggest that TRAF2 RING domain binds to phospholipids (e.g., PI3P) and that Ser-11 phosphorylation interferes with the interaction between the RING domain and phospholipids.

DISCUSSION

The signaling pathways downstream from the CD40L-CD40 axis have been extensively studied because of their important roles in the modulation of humoral and cellular immunity. Under physiological conditions, CD40 is expressed by antigen-presenting cells, such as B cells, macrophages, and dendritic cells, while CD40L is expressed by activated T cells and platelets (1). CD40L can be shed from T cells and platelets in a soluble form (sCD40L; also known as sCD154). Under pathological conditions, such as inflammation and malignant transformation, CD40 is inducibly expressed by endothelial cells, fibroblasts, and cancer cells and CD40L is expressed by monocytes and B cells (38, 39). These pathophysiological expressions of CD40 and CD40L have been implicated in a variety of immune-mediated inflammatory diseases (IMIDs), such as atherosclerosis, rheumatoid arthritis, alloimmune injury, and tumor progression (11, 38). Consequently, CD40-CD40L interaction has been targeted in IMIDs using humanized anti-CD40L monoclonal antibodies; however, the clinical trials were halted due to the incidence of thromboembolic events (38–40). Nevertheless, because of the critical roles of CD40 signaling in the regulation of immune responses, alternative strategies targeting CD40 signaling are still considered attractive approaches. To do so, it is important to understand the mechanistic details of the pathway activation.

Upon ligation, CD40 recruits TRAFs to rapidly activate the canonical NF-κB and MAPK (e.g., JNK) pathways (41). However, the spatiotemporal regulation of activation of the NF-κB and JNK pathways has been elusive. We have identified TRAF2 phosphorylation sites (Ser-11 and Ser-55) and reported that TRAF2 phosphorylation promotes the activation of the secondary/prolonged phase of the IKK and JNK pathways following TNF-α stimulation (22, 23). In the current study, TRAF2 Ser-11 phosphorylation was also found to be required for the secondary phase of IKK activation in response to CD40 ligation. With respect to JNK activation, both the early and secondary phases of JNK activation were suppressed but not completely impaired in TRAF2-S11A-expressing

cells. In addition, while no defects were observed in IκBα or IP-10 induction in TRAF2-S11A cells, RANTES and CD80 expression was significantly decreased compared to their expression in the TRAF2-WT counterparts. Analysis of the signaling complex localization in the cells revealed that TRAF2 Ser-11 phosphorylation is required for the translocation of the signaling complex from CD40 to the cytoplasm. Notably, early response genes, such as the IP-10 and IκBα genes, tend to have open promoters that are easily accessible to transcription factors to provide for their rapid induction upon transient NF-κB activation. In contrast, others require activation-dependent chromatin modifications for the transcription factors to access gene promoters, and thus, prolonged NF-κB activation is necessary for their efficient expression (42, 43). Thus, our findings reveal a new layer of regulation whereby TRAF2 Ser-11 phosphorylation-mediated cytoplasmic translocation of the signaling complex promotes JNK and IKK activation to regulate the expression of a subset of NF-κB target genes that require prolonged IKK/NF-κB activation following CD40 ligation.

Notably, some (e.g., TRAF2, TRAF3, and cIAP1/2) but not all components of the CD40 signaling complex are known to translocate to the lipid rafts following ligation, and this translocation is dependent on the TRAF2 RING domain (16, 44, 45). Chaudhuri et al. reported that TRAF2 is phosphorylated on serine residues and that this phosphorylation inhibits TRAF2 interaction with the cytoplasmic domain of CD40 (20, 21). However, in these studies, the authors neither identified TRAF2 phosphorylation sites nor analyzed the direct interaction between the CD40 cytoplasmic domain and phosphorylated TRAF2 (phospho-TRAF2); instead, they showed by *in vivo* [^{32}P]orthophosphate labeling experiments that phosphorylated TRAF2 dissociates from CD40. Our *in vivo* [^{32}P]orthophosphate labeling experiments in the same cells with the same conditions reveal that mutation of Ser-11 to Ala suppresses the overall ^{32}P-labeled-TRAF2 signal by 90% (22, 23), suggesting that Chaudhuri et al. were in fact also monitoring TRAF2 Ser-11 phosphorylation in their experiments. TRAF2 Ser-11 phosphorylation occurs in its N-terminal region, but TRAF2 interacts with the cytoplasmic tail of CD40 via its C-terminal TRAF domain; thus, it is unlikely that TRAF2 Ser-11 phosphorylation directly triggers the dissociation of TRAF2 from CD40. Our IF staining data reveal that TRAF2-S11A partially localizes to MVBs and deletion of the RING domain prevents MVB localization. Protein-lipid overlay and lipid affinity matrix pulldown assays revealed that the TRAF2 RING domain interacts with phospholipids (e.g., PI3P) and Ser-11 phosphorylation inhibits this interaction. These published findings and our data suggest that TRAF2 Ser-11 phosphorylation inhibits the interaction between the TRAF2 RING domain and phospholipids to block the translocation of TRAF2 to lipid rafts and caveosomes, which allows the TRAF2-associated signaling complex to translocate from CD40 to the cytoplasm. In the absence of TRAF2 Ser-11 phosphorylation, the RING-phospholipid interaction retains TRAF2 and TRAF2-associated proteins in the membrane, which facilitates the eventual translocation of TRAF2 and TRAF2-associated proteins to lipid rafts and MVBs.

S1P has been shown to bind the TRAF2 RING domain to promote its E3 ligase activity (5). This finding prompted us to speculate that TRAF2 phosphorylation may also promote its E3 ligase activity. Therefore, in the past several years, we have extensively analyzed the possible roles of TRAF2 phosphorylation in its E3 ligase activity. We expressed and purified WT and phosphomimetic forms of TRAF2 protein from *E. coli*, Sf9, and 293T cells and carried out *in vitro* ubiquitination assays in the presence of UbcH5a/b or Ubc13/UevA. However, we have never been able to show TRAF2 E3 ligase activity *in vitro* (unpublished observations). We also examined TRAF2 E3 ligase activity in the presence or absence of phospholipids (e.g., PI3P and S1P), but again we were not able to see any TRAF2 E3 ligase activity. Recent structural and biochemical analyses reveal that the TRAF2 RING domain does not interact with E2s (46). TRAF2 constitutively interacts with cIAP1/2 (potent E3 ligases) in the cytoplasm and recruits them to several members of the TNFR superfamily. Recently, an increasing body of studies has revealed that cIAP1/2 but not TRAF2 directly catalyze K63-linked ubiquitination of effector proteins (9, 44, 45). These observations suggest that catalysis of ubiquitination may not

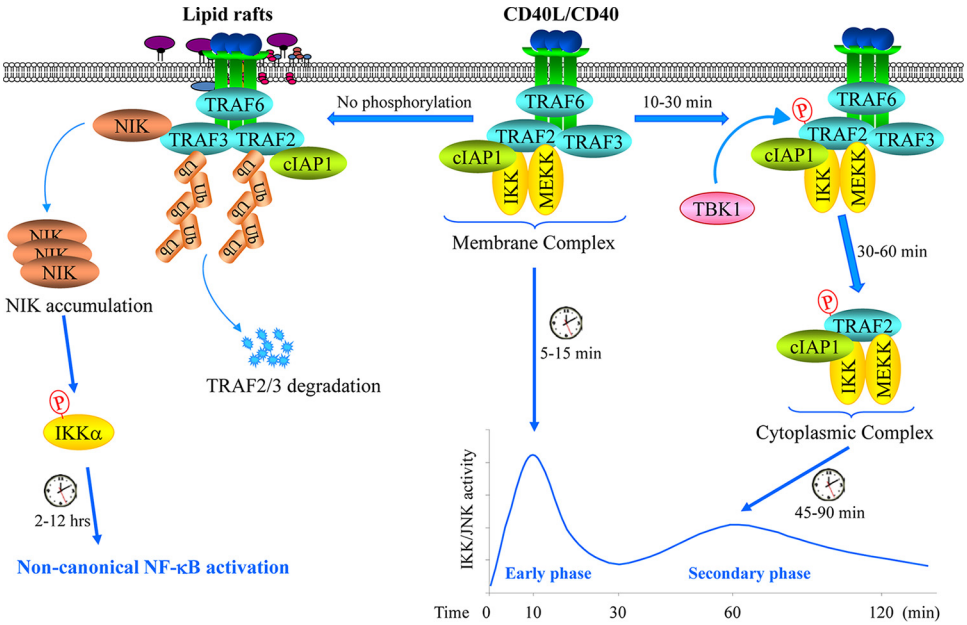

FIG 9 A possible model for the CD40 signaling mechanisms. Upon ligation, CD40 recruits TRAF6, TRAF3, TRAF2, cIAP1, IKK, and MEKK to initiate the immediate phases of IKK and JNK activation within 10 min. Thereafter, if TRAF2 is phosphorylated on Ser-11 by TBK1, the TRAF2-cIAP1-IKK-MEKK complex dissociates from CD40 and translocates to the cytoplasm to initiate the secondary/prolonged phases of IKK and JNK activation within 45 to 90 min; if TRAF2 is not phosphorylated, the TRAF2-associated complex then translocates to lipid rafts where TRAF2 and TRAF3 are degraded, resulting in NIK protein accumulation and NIK-dependent activation of the noncanonical NF-κB pathway within 2 to 12 h after ligation.

be the function of the TRAF2 RING domain in signal transduction. Our *in vivo* and *in vitro* data reveal that (i) the TRAF2 RING domain is essential for TRAF2 localization to MVBs in the cells, (ii) the TRAF2 RING domain binds phospholipids *in vitro*, which is inhibited by TRAF2 Ser-11 phosphorylation, and (iii) in TRAF2-S11A-expressing cells, TRAF2 and TRAF2-associated proteins remain in the membrane/lipid raft fractions following CD40 ligation and the secondary phase of JNK and IKK activation is impaired. These data suggest that the functions of the TRAF2 RING domain and Ser-11 phosphorylation are most likely to control TRAF2-phospholipid interaction to regulate the destiny of the signaling complex and, thereby, the secondary phase of JNK and IKK activation in response to CD40 ligation.

In unstimulated cells, TRAF2, cIAP1/2, and TRAF3 cooperatively target NIK for ubiquitination and degradation to suppress noncanonical NF-κB pathway activation (12). Recently, TBK1 was shown to negatively regulate noncanonical NF-κB activation and IgA class switching; in TBK1-KO B cells, noncanonical NF-κB is constitutively activated to a certain degree (47). However, the mechanisms by which TBK1 suppresses the noncanonical NF-κB pathway have been unclear. Shen et al. have reported that IKKε (a homologous kinase of TBK1) directly phosphorylates TRAF2 at Ser-11 to promote canonical NF-κB activation (28). We found that TBK1 directly phosphorylates Ser-11 in response to CD40 ligation and that this phosphorylation plays an essential role in suppression of the noncanonical NF-κB activation. In the absence of TRAF2 Ser-11 phosphorylation, a significant portion of cIAP1/2 were recruited to the membrane/lipid raft fractions by TRAF2, resulting in constitutive noncanonical NF-κB activation. Thus, our findings provide a mechanism whereby TBK1-mediated TRAF2 Ser-11 phosphorylation serves as a molecular switch to control the bifurcation of canonical and noncanonical NF-κB activation.

In summary, our data reveal a new model for the role of the TRAF2 RING domain and Ser-11 phosphorylation (Fig. 9). (i) Upon CD40 ligation, TRAF2 is recruited to the CD40 receptor complex independent of its RING domain and Ser-11 phosphorylation; (ii) TBK1 directly phosphorylates TRAF2 at Ser-11 within the CD40 signaling complex; (iii)

Ser-11 phosphorylation inhibits TRAF2 RING interaction with phospholipids, allowing TRAF2-associated proteins to translocate from CD40 to the cytoplasm to promote JNK and canonical NF-κB activation; and (iv) in the absence of Ser-11 phosphorylation, the TRAF2 complex translocates to the lipid rafts and then internalizes and gets degraded, resulting in noncanonical NF-κB activation.

MATERIALS AND METHODS

Cell lines and medium. The A20.2J and CH12.LX mouse B cell lymphoma lines and their TRAF2 knockout (TRAF2-KO) subclones have been described previously (35, 44). TRAF2-deficient human HAP1 cells (catalog ID: HZGHC002588c010) generated by clustered regularly interspaced short palindromic repeat (CRISPR)-CRISPR-associated protein 9 (Cas9)-mediated knockout were purchased from Horizon Discovery (Cambridge, UK). These cell lines were maintained in RPMI 1640 (Gibco, Grand Island, NY) supplemented with 10% heat-inactivated fetal bovine serum (HI-FBS) (Atlanta Biologicals, Atlanta, GA), 10 μM β-mercaptoethanol (Gibco), and 1× penicillin-streptomycin (Gibco). Wild-type (WT) and TBK1/IKKε DKO MEFs were kindly provided by Shizuo Akira and Takashi Satoh (Osaka University, Osaka, Japan) and cultured in Dulbecco's modified Eagle's medium (DMEM) supplemented with 10% bovine calf serum, nonessential amino acids (Gibco), and 1× penicillin-streptomycin (Gibco), as described previously (48, 49).

Antibodies and reagents. Antibodies were purchased as follows: anti-TRAF2 (C-20; sc-876), anti-TRAF3 (H-122; sc1828), anti-JNK (FL; sc-571), anti-MEKK1 (C-22; sc-252), anti-IKKα/β (H-470; sc-7607), anti-IKKγ (FL-419; sc-8330), and anti-ASK1 (H-300; sc-7931) antibodies (Abs) were from Santa Cruz Biotechnology, Inc. (Dallas, TX). Anti-TBK1 (D1B4), anti-phospho-IKKα/β (Ser176/180; 16A6), anti-IκBα (9242), anti-phospho-p65 (Ser536; 3031), anti-p65 (3031), anti-p100/52 (NF-κB2; 4882), and anti-flotillin-2 (C42A3; 3436) Abs were from Cell Signaling (Beverly, MA). Anti-phospho-JNK Ab was from Promega (Madison, WI), anti-pan-cIAP Ab was from R&D Systems (Minneapolis, MN), antiubiquitin Ab was from Boston Biochem, Inc. (Cambridge, MA), anti-RIP1 Ab was from BD Biosciences (San Jose, CA), and anti-TRAIL-R1 (catalog number 556544; DR4) and anti-β-tubulin (E7) Abs were from the University of Iowa Developmental Studies Hybridoma Bank. Anti-TRAF2 Ser-11 phospho-Ab is custom-made and has been reported previously (22, 23). The G28.5 (mouse IgG1 anti-human CD40) and 1C10 (rat IgG2a anti-mouse) monoclonal Abs were produced from hybridoma lines purchased from ATCC (HB-9110; Manassas, VA) and provided by Frances Lund (University of Alabama, Birmingham) (50) and were purified by ammonium sulfate precipitation and dialysis against phosphate-buffered saline (PBS) as described previously (50, 51). Mouse-specific MegaCD40L was purchased from Enzo Life Sciences (Farmingdale, NY). Protease/phosphatase inhibitor cocktail was purchased from Pierce (Rockford, IL). BX-795 was purchased from Cayman Chemical (Ann Arbor, MI), and PKC inhibitors (Gö6976 and Gö6983) were from Selleck Chemical (Houston, TX).

Primary cell isolation. Human $CD19^+$ $CD43^-$ resting B cells were purified from peripheral blood mononuclear cells (PBMCs) isolated from a leukocyte reduction system (LRS) cone (DeGowin Blood Center, University of Iowa Hospitals and Clinics, Iowa City, IA) using Ficoll-Paque separation medium (GE Healthcare, Piscataway, NJ) as previously described (52), followed by negative selection with the magnetically activated cell sorting (MACS) human B cell isolation kit II and LS columns (Miltenyi Biotech, Inc., Auburn, CA) according to the manufacturer's protocol. Splenocytes were isolated from 8-week-old female C57BL/6 mice by Ficoll-Paque density centrifugation and used to isolate splenic B cells by negative selection with a MACS mouse B cell isolation kit and LS columns (Miltenyi Biotech, Inc.). Bone marrow-derived macrophages (BMDMs) were prepared from bone marrow cells isolated from the femurs and tibias of 6- to 8-week-old C57BL/6 mice. Bone marrow cells were seeded at 2×10^6 cells/ml and cultured in L929-conditioned RPMI 1640 medium for 7 days. Adherent and fully differentiated macrophages were further cultured in unconditioned medium for 72 h prior to stimulation with 1C10 Ab on postisolation day 10.

Plasmids. Retroviral expression vectors of TRAF2-WT and -S11A (pBabe-TRAF2 and pQCXIH-TRAF2) and pcDNA3 vectors of constitutively active (CA) forms of PKCα, PKCε, PKCζ, and Myr-AKT1 have been reported previously (53–55). pCDNA3-EGFP-TRAF2-Δ1-18 was constructed by subcloning TRAF2-Δ1-18 to pCDNA3-EGFP. Rab5a-pmCherryC1, Lamp1-RFP, and caveolin-1–mRFP (Cav1-mRFP) were from Addgene (56–58). To knock down MEKK1 and TBK1, three sets of shRNAs were designed for mouse MEKK1 and TBK1 and inserted into the BamHI and EcoRI sites of the pLSLPw vector; the shRNA sequence that worked best for TBK1 (accession number NM_019786) was CCAGAATCAGAATTTCTCATT, and the one that worked best for MEKK1 (accession number AF117340) was CTTTGTCTCATGCTCAATTAA. The human CD40 expression vector was created by subcloning the hCD40 cDNA into the pQCXIP retroviral vector.

Retroviral transduction. 293T cells were seeded at 1.5×10^6 per 10-cm plate and on the next day cotransfected with 2 μg each of pMD.OGP (encoding Gag-Pol), pMD.G (encoding vesicular stomatitis virus G protein [VSV-G]), and pBabe-TRAF2-WT/S11A or pQCXIH-TRAF2-WT/S11A by a standard calcium phosphate precipitation method. Viral supernatant was collected 48 h after transfection and centrifuged at 2,000 × *g* for 10 min to remove cell debris. Viral supernatant was then diluted 2-, 3-, 4-, and 5-fold with RPMI 1640 containing 10% HI-FBS and used immediately for infections of A20.2J-TRAF2-KO and CH12.LX-TRAF2-KO B cell lymphoma lines in 24-well plates in the presence of 10 μg/ml Polybrene by a general spin infection (spinfection) protocol (e.g., spinning at 1,250 × *g* for 90 min at room temperature). At 24 h after infection, cells were selected with puromycin or hygromycin for 10 or 14 days, respectively. Resistant cells were then analyzed for TRAF2 expression by Western blotting. Those with physiological gene expression levels (transduced with retroviral supernatant at a 4-fold dilution) were used for the functional experiments within 1 month after selection.

Western blotting. Cells were treated as indicated in the figures and figure legends, and protein samples were extracted with a high-salt lysis buffer (350 mM NaCl, 20% glycerol, 0.5% Triton X-100, 2 mM EDTA, 1 mM dithiothreitol [DTT], 25 mM Tris-HCl, pH 7.4) supplemented with a cocktail of protease and phosphatase inhibitors for 30 min on ice and then centrifuged at 13,000 × *g* for 20 min. Cleared lysates were subjected to protein quantification by Bradford assay, and 20 μg protein was separated by SDS-PAGE and transferred onto nitrocellulose membranes. For phosphorylated-protein detection, blots were blocked with Tris-buffered saline (TBS) supplemented with 0.2% Tween 20 (TTBS) and 3% bovine serum albumin (BSA) for 4 h prior to incubation with primary Ab overnight at 4°C. For non-phosphorylated-protein detection, blots were blocked with TTBS supplemented with 5% fat-free milk. Proteins were then visualized with horseradish peroxidase-labeled secondary antibodies (Jackson ImmunoResearch, West Grove, PA) and enhanced chemiluminescence (ECL) solution as previously described (54). Densitometric analysis was performed with Image Studio software (LI-COR Biosciences, Lincoln, NE).

Real-time quantitative reverse transcription-PCR (qRT-PCR). A20.2J-TRAF2-KO cells stably expressing TRAF2-WT or TRAF2-S11A were treated with pretrimerized MegaCD40L (100 μg/ml) as indicated, and the total RNA was extracted using the RNeasy minikit (Qiagen). Five micrograms of RNA was treated with RQ1 RNase-free DNase for 30 min at 37°C and reverse transcribed using an oligo(dT) primer. The resulting cDNA was then subjected to quantitative PCR using the Power master mix and an ABI Prism 7700 sequence detector (Applied Biosystems). Mouse glyceraldehyde-3-phosphate dehydrogenase (GAPDH)-specific primers were used to generate an internal control, and the average threshold cycle (C_T) for samples in triplicate was used in the subsequent calculations. Relative expression levels of NF-κB target genes were calculated as the ratios with respect to the GAPDH expression level. Real-time PCR products were also separated on an agarose gel to confirm the presence of single bands (data not shown). All primer pair sets were designed to flank an intron and have been reported previously (53, 54).

Subcellular fractionation. To prepare soluble and insoluble fractions, cells were harvested with ice-cold PBS and lysed in gentle lysis buffer (G-LB; 100 mM NaCl, 10% glycerol, 0.25% Triton X-100, 1 mM EDTA, 1 mM DTT, 25 mM Tris-HCl [pH 7.4], and 1× protease/phosphatase inhibitors) on ice for 30 min, followed by a 15-min centrifugation at 13,000 × *g*. The resulting supernatants were taken as the soluble fraction. The pellets were then washed once with PBS, lysed in radioimmunoprecipitation assay (RIPA) buffer for 20 min on ice, and centrifuged at 13,000 × *g* for 15 min, and the supernatants were taken as the insoluble fraction. For the membrane and cytoplasmic fractionations, cell pellets were incubated in hypotonic buffer (20 mM HEPES-KOH [pH 7.4], 10 mM NaCl, 3 mM $MgCl_2$, 1 mM DTT, and 1× protease/phosphatase inhibitors) for 15 min on ice prior to disruption with a Dounce homogenizer and then centrifuged at 500 × *g* for 10 min to remove nuclei and unbroken cells. The supernatants were then centrifuged at 12,000 × *g* for 10 min, and the resulting supernatants were taken as cytoplasmic protein. The membrane pellets were rinsed once in PBS, lysed in RIPA buffer for 30 min on ice, and centrifuged at 13,000 × *g* for 15 min, and the supernatants were taken as the membrane fraction.

Coimmunoprecipitation. Cells were stimulated with 1C10 Ab (rat IgG) and harvested with ice-cold PBS. Cell pellets were then lysed in immunoprecipitation buffer (IP-LB; 20 mM Tris-HCl [pH 7.4], 135 mM NaCl, 2 mM EDTA, 2 mM EGTA, 1% Triton X-100, 10% glycerol, 1 mM DTT, and 1× protease/phosphatase inhibitors) for 30 min on ice and cleared by centrifugation at 13,000 × *g* for 15 min. The 1C10/CD40 receptor complex was immunoprecipitated first with protein G-agarose beads (Thermo Scientific, Waltham, MA) precoated with goat anti-rat IgG (Jackson ImmunoResearch) for 2 h, rotating end over end at 4°C. After the beads were pelleted, the supernatants containing the cytoplasmic TRAF2 complexes were immunoprecipitated with protein G beads precoated with anti-TRAF2 Ab for 2 h at 4°C with constant rotation. The protein-bound beads were then washed three times with IP-LB prior to elution with 2× SDS-sample buffer for 5 min at 95°C, followed by Western blotting analysis.

Flow cytometry. WT and TBK1/IKKε DKO MEFs were infected with pBabe-hCD40 (human CD40) retroviral supernatants in the presence of 4 μg/ml Polybrene for 6 h. At 48 h after infection, the MEFs were selected with puromycin (2.0 μg/ml) for 7 days, and resistant cells were pooled and cultured for 2 days without puromycin. The MEFs were then stained with allophycocyanin (APC)-conjugated anti-hCD40 Ab (Biolegend, San Diego, CA) and analyzed with fluorescence-activated cell sorting (FACS; Becton Dickinson FACSCanto II), following the manufacturer's protocol, to confirm CD40 cell surface expression.

Immunofluorescence microscopy. HeLa cells and MEFs grown on glass coverslips were transfected with indicated plasmids using Lipofectamine 2000 reagent (Invitrogen) according to the manufacturer's protocol. Thirty-six hours after transfection, the cells were fixed, permeabilized, blocked, and incubated with anti-FLAG or anti-TRAF2 Ab (1:1,000 dilutions) in 3% BSA-PBS as described previously (59). The cells were then washed three times with PBS and exposed to Alexa Fluor 488-conjugated anti-mouse or anti-rabbit IgG (1:1,000 dilution; Molecular Probes) for 1 h at room temperature to label TRAF2, after which they were stained with DAPI (4′,6-diamidino-2-phenylindole) for 2 min to label nuclei. After further washes, coverslips were mounted on glass slides, and TRAF2 and nuclei were visualized under an immunofluorescence microscope.

Sucrose gradient isolation of lipid rafts. 293T cells were transfected with TRAF2-WT/S11A-FLAG (1.0 μg), and 36 h after transfection, the cells were harvested with ice-cold PBS and lysed in 0.5 ml of gentle lysis buffer (G-LB) on ice for 20 min. The same amount of 80% sucrose in G-LB (Triton X-100 free) was added and mixed in, and the mixture was transferred to a centrifuge tube. The sample was then sequentially overlaid with 2 ml of 30% sucrose and 1 ml of 5% sucrose in G-LB (Triton X-100 free) and centrifuged at 200,000 × *g* in a Beckman (SW60 Ti) centrifuge for 16 h. The opaque band migrating between 5% and 30% sucrose (light buoyant lipid rafts) was harvested, diluted with detergent-free G-LB,

and pelleted by centrifugation at 13,000 × g for 10 min. The pellets were then solubilized in RIPA buffer by sonication and subjected to Western blot analysis for TRAF2 expression.

Lipid-protein overlay assays. Lipid-protein overlay assays were performed with Membrane Lipid Strips purchased from Echelon Biosciences, Inc. (Salt Lake City, UT), using the manufacturer's protocol. Briefly, GST-TRAF2$^{1-128}$ and TRAF2$^{1-133}$-His fusion proteins were expressed and purified from *E. coli* cells and then dialyzed against TBS containing 0.25% Triton X-100 (TBS-T). The Membrane Lipid Strips, spotted with 100 pmol of biologically relevant membrane lipids, were blocked for 1 h in TBS-T containing 3% BSA prior to incubation with fusion proteins (0.5 μg/ml in TBS-T–3% BSA) for 90 min at room temperature. Following extensive washing, bound proteins were detected by immunoblotting with anti-GST or anti-TRAF2 N-terminal Ab.

Statistical analysis. Data represent the mean values ± standard deviations (SD) from at least three independent experiments. All statistical analyses were performed with Prism 6 (GraphPad Software, La Jolla, CA). Statistical comparisons were made with two-tailed unpaired *t* tests unless otherwise noted. A *P* value of <0.05 was considered statistically significant.

ACKNOWLEDGMENTS

We thank Siegfried Janz, Jon Houtman, and John Colgan (University of Iowa) for their insightful discussion, Gail Bishop and Bruce Hostager (University of Iowa) for generously providing us with TRAF2-deficient A20.2J and CH12.LX cells, Shizuo Akira and Takashi Satoh (Osaka University, Osaka, Japan) for WT and TBK1/IKKε DKO MEFs, and Frances Lund (University of Alabama, Birmingham) for providing us with 1C10 hybridoma. Leukocyte reduction system (LRS) cones were provided by the DeGowin Blood Center at the University of Iowa Hospitals and Clinics. The β-tubulin (E7) monoclonal antibody was developed by M. Klymkowski and obtained from the Developmental Studies Hybridoma Bank developed under the auspices of the NICHD and maintained by the Department of Biology at the University of Iowa.

Supports by NCI grant CA138475 and DOD grant BC141753 (to H.H.) are gratefully acknowledged.

All authors have declared no conflicts of interest.

REFERENCES

1. Bishop GA. 2004. The multifaceted roles of TRAFs in the regulation of B-cell function. Nat Rev Immunol 4:775–786. https://doi.org/10.1038/nri1462.
2. Graham JP, Arcipowski KM, Bishop GA. 2010. Differential B-lymphocyte regulation by CD40 and its viral mimic, latent membrane protein 1. Immunol Rev 237:226–248. https://doi.org/10.1111/j.1600-065X.2010.00932.x.
3. Ha H, Han D, Choi Y. 2009. TRAF-mediated TNFR-family signaling. Curr Protoc Immunol 11:Unit 11.19D. https://doi.org/10.1002/0471142735.im1109ds87.
4. Chen ZJ, Sun LJ. 2009. Nonproteolytic functions of ubiquitin in cell signaling. Mol Cell 33:275–286. https://doi.org/10.1016/j.molcel.2009.01.014.
5. Alvarez SE, Harikumar KB, Hait NC, Allegood J, Strub GM, Kim E, Maceyka M, Jiang H, Luo C, Kordula T, Milstien S, Spiegel S. 2010. Sphingosine-1-phosphate: a missing cofactor for the E3 ubiquitin ligase TRAF2. Nature 465:1084–1088. https://doi.org/10.1038/nature09128.
6. Habelhah H, Takahashi S, Cho SG, Kadoya T, Watanabe T, Ronai Z. 2004. Ubiquitination and translocation of TRAF2 is required for activation of JNK but not of p38 or NF-kappaB. EMBO J 23:322–332. https://doi.org/10.1038/sj.emboj.7600044.
7. Lamothe B, Campos AD, Webster WK, Gopinathan A, Hur L, Darnay BG. 2008. The RING domain and first zinc finger of TRAF6 coordinate signaling by interleukin-1, lipopolysaccharide, and RANKL. J Biol Chem 283:24871–24880. https://doi.org/10.1074/jbc.M802749200.
8. Napetschnig J, Wu H. 2013. Molecular basis of NF-kappaB signaling. Annu Rev Biophys 42:443–468. https://doi.org/10.1146/annurev-biophys-083012-130338.
9. Vince JE, Pantaki D, Feltham R, Mace PD, Cordier SM, Schmukle AC, Davidson AJ, Callus BA, Wong WW, Gentle IE, Carter H, Lee EF, Walczak H, Day CL, Vaux DL, Silke J. 2009. TRAF2 must bind to cellular inhibitors of apoptosis for tumor necrosis factor (TNF) to efficiently activate NF-{kappa}B and to prevent TNF-induced apoptosis. J Biol Chem 284:35906–35915. https://doi.org/10.1074/jbc.M109.072256.
10. Zhang L, Blackwell K, Shi Z, Habelhah H. 2010. The RING domain of TRAF2 plays an essential role in the inhibition of TNFalpha-induced cell death but not in the activation of NF-kappaB. J Mol Biol 396:528–539. https://doi.org/10.1016/j.jmb.2010.01.008.
11. Elgueta R, Benson MJ, de Vries VC, Wasiuk A, Guo Y, Noelle R. 2009. Molecular mechanism and function of CD40/CD40L engagement in the immune system. Immunol Rev 229:152–172. https://doi.org/10.1111/j.1600-065X.2009.00782.x.
12. Vallabhapurapu S, Matsuzawa A, Zhang W, Tseng PH, Keats JJ, Wang H, Vignali DA, Bergsagel PL, Karin M. 2008. Nonredundant and complementary functions of TRAF2 and TRAF3 in a ubiquitination cascade that activates NIK-dependent alternative NF-kappaB signaling. Nat Immunol 9:1364–1370. https://doi.org/10.1038/ni.1678.
13. Zarnegar BJ, Wang Y, Mahoney DJ, Dempsey PW, Cheung HH, He J, Shiba T, Yang X, Yeh WC, Mak TW, Korneluk RG, Cheng G. 2008. Noncanonical NF-kappaB activation requires coordinated assembly of a regulatory complex of the adaptors cIAP1, cIAP2, TRAF2 and TRAF3 and the kinase NIK. Nat Immunol 9:1371–1378. https://doi.org/10.1038/ni.1676.
14. Matsuzawa A, Tseng PH, Vallabhapurapu S, Luo JL, Zhang W, Wang H, Vignali DA, Gallagher E, Karin M. 2008. Essential cytoplasmic translocation of a cytokine receptor-assembled signaling complex. Science 321:663–668. https://doi.org/10.1126/science.1157340.
15. Brown KD, Hostager BS, Bishop GA. 2001. Differential signaling and TRAF degradation by CD40 and the EBV oncoprotein LMP1. J Exp Med 193:943–954. https://doi.org/10.1084/jem.193.8.943.
16. Brown KD, Hostager BS, Bishop GA. 2002. Regulation of TRAF2 signaling by self-induced degradation. J Biol Chem 277:19433–19438. https://doi.org/10.1074/jbc.M111522200.
17. Moore CR, Bishop GA. 2005. Differential regulation of CD40-mediated TNF receptor-associated factor degradation in B lymphocytes. J Immunol 175:3780–3789. https://doi.org/10.4049/jimmunol.175.6.3780.
18. Lin WW, Hildebrand JM, Bishop GA. 2013. A complex relationship between TRAF3 and non-canonical NF-kappaB2 activation in B lymphocytes. Front Immunol 4:477. https://doi.org/10.3389/fimmu.2013.00477.
19. Hostager BS, Bishop GA. 2013. CD40-mediated activation of the NF-kappaB2 pathway. Front Immunol 4:376. https://doi.org/10.3389/fimmu.2013.00376.
20. Chaudhuri A, Orme S, Eilam S, Cherayil BJ. 1997. CD40-mediated signals inhibit the binding of TNF receptor-associated factor 2 to the CD40 cytoplasmic domain. J Immunol 159:4244–4251.

21. Chaudhuri A, Orme S, Vo T, Wang W, Cherayil BJ. 1999. Phosphorylation of TRAF2 inhibits binding to the CD40 cytoplasmic domain. Biochem Biophys Res Commun 256:620–625. https://doi.org/10.1006/bbrc.1999.0385.
22. Blackwell K, Zhang L, Thomas GS, Sun S, Nakano H, Habelhah H. 2009. TRAF2 phosphorylation modulates tumor necrosis factor alpha-induced gene expression and cell resistance to apoptosis. Mol Cell Biol 29:303–314. https://doi.org/10.1128/MCB.00699-08.
23. Thomas GS, Zhang L, Blackwell K, Habelhah H. 2009. Phosphorylation of TRAF2 within its RING domain inhibits stress-induced cell death by promoting IKK and suppressing JNK activation. Cancer Res 69:3665–3672. https://doi.org/10.1158/0008-5472.CAN-08-4867.
24. Vallabhapurapu S, Karin M. 2009. Regulation and function of NF-kappaB transcription factors in the immune system. Annu Rev Immunol 27:693–733. https://doi.org/10.1146/annurev.immunol.021908.132641.
25. Moscat J, Diaz-Meco MT, Rennert P. 2003. NF-kappaB activation by protein kinase C isoforms and B-cell function. EMBO Rep 4:31–36. https://doi.org/10.1038/sj.embor.embor704.
26. Bonnard M, Mirtsos C, Suzuki S, Graham K, Huang J, Ng M, Itie A, Wakeham A, Shahinian A, Henzel WJ, Elia AJ, Shillinglaw W, Mak TW, Cao Z, Yeh WC. 2000. Deficiency of T2K leads to apoptotic liver degeneration and impaired NF-kappaB-dependent gene transcription. EMBO J 19:4976–4985. https://doi.org/10.1093/emboj/19.18.4976.
27. Leitges M, Sanz L, Martin P, Duran A, Braun U, Garcia JF, Camacho F, Diaz-Meco MT, Rennert PD, Moscat J. 2001. Targeted disruption of the zetaPKC gene results in the impairment of the NF-kappaB pathway. Mol Cell 8:771–780. https://doi.org/10.1016/s1097-2765(01)00361-6.
28. Shen RR, Zhou AY, Kim E, Lim E, Habelhah H, Hahn WC. 2012. IkappaB kinase epsilon phosphorylates TRAF2 to promote mammary epithelial cell transformation. Mol Cell Biol 32:4756–4768. https://doi.org/10.1128/MCB.00468-12.
29. Saccani S, Pantano S, Natoli G. 2001. Two waves of nuclear factor kappaB recruitment to target promoters. J Exp Med 193:1351–1359. https://doi.org/10.1084/jem.193.12.1351.
30. Schmidt C, Peng B, Li Z, Sclabas GM, Fujioka S, Niu J, Schmidt-Supprian M, Evans DB, Abbruzzese JL, Chiao PJ. 2003. Mechanisms of proinflammatory cytokine-induced biphasic NF-kappaB activation. Mol Cell 12:1287–1300. https://doi.org/10.1016/s1097-2765(03)00390-3.
31. Werner SL, Barken D, Hoffmann A. 2005. Stimulus specificity of gene expression programs determined by temporal control of IKK activity. Science 309:1857–1861. https://doi.org/10.1126/science.1113319.
32. Hoffmann A, Natoli G, Ghosh G. 2006. Transcriptional regulation via the NF-kappaB signaling module. Oncogene 25:6706–6716. https://doi.org/10.1038/sj.onc.1209933.
33. Baccam M, Bishop GA. 1999. Membrane-bound CD154, but not CD40-specific antibody, mediates NF-kappaB-independent IL-6 production in B cells. Eur J Immunol 29:3855–3866. https://doi.org/10.1002/(SICI)1521-4141(199912)29:12<3855::AID-IMMU3855>3.0.CO;2-S.
34. Fotin-Mleczek M, Henkler F, Hausser A, Glauner H, Samel D, Graness A, Scheurich P, Mauri D, Wajant H. 2004. Tumor necrosis factor receptor-associated factor (TRAF) 1 regulates CD40-induced TRAF2-mediated NF-kappaB activation. J Biol Chem 279:677–685. https://doi.org/10.1074/jbc.M310969200.
35. Hostager BS, Haxhinasto SA, Rowland SL, Bishop GA. 2003. Tumor necrosis factor receptor-associated factor 2 (TRAF2)-deficient B lymphocytes reveal novel roles for TRAF2 in CD40 signaling. J Biol Chem 278:45382–45390. https://doi.org/10.1074/jbc.M306708200.
36. Tibbetts MD, Shiozaki EN, Gu L, McDonald ER, III, El-Deiry WS, Shi Y. 2004. Crystal structure of a FYVE-type zinc finger domain from the caspase regulator CARP2. Structure 12:2257–2263. https://doi.org/10.1016/j.str.2004.10.007.
37. Rusten TE, Stenmark H. 2006. Analyzing phosphoinositides and their interacting proteins. Nat Methods 3:251–258. https://doi.org/10.1038/nmeth867.
38. Loskog AS, Eliopoulos AG. 2009. The Janus faces of CD40 in cancer. Semin Immunol 21:301–307. https://doi.org/10.1016/j.smim.2009.07.001.
39. Vonderheide RH. 2007. Prospect of targeting the CD40 pathway for cancer therapy. Clin Cancer Res 13:1083–1088. https://doi.org/10.1158/1078-0432.CCR-06-1893.
40. Khalil M, Vonderheide RH. 2007. Anti-CD40 agonist antibodies: preclinical and clinical experience. Update Cancer Ther 2:61–65. https://doi.org/10.1016/j.uct.2007.06.001.
41. Bishop GA, Moore CR, Xie P, Stunz LL, Kraus ZJ. 2007. TRAF proteins in CD40 signaling. Adv Exp Med Biol 597:131–151. https://doi.org/10.1007/978-0-387-70630-6_11.
42. Smale ST. 2010. Selective transcription in response to an inflammatory stimulus. Cell 140:833–844. https://doi.org/10.1016/j.cell.2010.01.037.
43. Fessele S, Maier H, Zischek C, Nelson PJ, Werner T. 2002. Regulatory context is a crucial part of gene function. Trends Genet 18:60–63. https://doi.org/10.1016/s0168-9525(02)02591-x.
44. Hostager BS, Catlett IM, Bishop GA. 2000. Recruitment of CD40 and tumor necrosis factor receptor-associated factors 2 and 3 to membrane microdomains during CD40 signaling. J Biol Chem 275:15392–15398. https://doi.org/10.1074/jbc.M909520199.
45. Varfolomeev E, Goncharov T, Maecker H, Zobel K, Komuves LG, Deshayes K, Vucic D. 2012. Cellular inhibitors of apoptosis are global regulators of NF-kappaB and MAPK activation by members of the TNF family of receptors. Sci Signal 5:ra22. https://doi.org/10.1126/scisignal.2001878.
46. Yin Q, Lamothe B, Darnay BG, Wu H. 2009. Structural basis for the lack of E2 interaction in the RING domain of TRAF2. Biochemistry 48:10558–10567. https://doi.org/10.1021/bi901462e.
47. Jin J, Xiao Y, Chang JH, Yu J, Hu H, Starr R, Brittain GC, Chang M, Cheng X, Sun SC. 2012. The kinase TBK1 controls IgA class switching by negatively regulating noncanonical NF-kappaB signaling. Nat Immunol 13:1101–1109. https://doi.org/10.1038/ni.2423.
48. Reilly SM, Chiang SH, Decker SJ, Chang L, Uhm M, Larsen MJ, Rubin JR, Mowers J, White NM, Hochberg I, Downes M, Yu RT, Liddle C, Evans RM, Oh D, Li P, Olefsky JM, Saltiel AR. 2013. An inhibitor of the protein kinases TBK1 and IKK-varepsilon improves obesity-related metabolic dysfunctions in mice. Nat Med 19:313–321. https://doi.org/10.1038/nm.3082.
49. Hemmi H, Takeuchi O, Sato S, Yamamoto M, Kaisho T, Sanjo H, Kawai T, Hoshino K, Takeda K, Akira S. 2004. The roles of two IkappaB kinase-related kinases in lipopolysaccharide and double stranded RNA signaling and viral infection. J Exp Med 199:1641–1650. https://doi.org/10.1084/jem.20040520.
50. Randall TD, Heath AW, Santos-Argumedo L, Howard MC, Weissman IL, Lund FE. 1998. Arrest of B lymphocyte terminal differentiation by CD40 signaling: mechanism for lack of antibody-secreting cells in germinal centers. Immunity 8:733–742. https://doi.org/10.1016/s1074-7613(00)80578-6.
51. Heath AW, Wu WW, Howard MC. 1994. Monoclonal antibodies to murine CD40 define two distinct functional epitopes. Eur J Immunol 24:1828–1834. https://doi.org/10.1002/eji.1830240816.
52. Dietz AB, Bulur PA, Emery RL, Winters JL, Epps DE, Zubair AC, Vuk-Pavlović S. 2006. A novel source of viable peripheral blood mononuclear cells from leukoreduction system chambers. Transfusion 46:2083–2089. https://doi.org/10.1111/j.1537-2995.2006.01033.x.
53. Zhang L, Blackwell K, Altaeva A, Shi Z, Habelhah H. 2011. TRAF2 phosphorylation promotes NF-kappaB-dependent gene expression and inhibits oxidative stress-induced cell death. Mol Biol Cell 22:128–140. https://doi.org/10.1091/mbc.E10-06-0556.
54. Zhang L, Blackwell K, Thomas GS, Sun S, Yeh WC, Habelhah H. 2009. TRAF2 suppresses basal IKK activity in resting cells and TNFalpha can activate IKK in TRAF2 and TRAF5 double knockout cells. J Mol Biol 389:495–510. https://doi.org/10.1016/j.jmb.2009.04.054.
55. Lopez-Bergami P, Habelhah H, Bhoumik A, Zhang W, Wang LH, Ronai Z. 2005. RACK1 mediates activation of JNK by protein kinase C. Mol Cell 19:309–320. https://doi.org/10.1016/j.molcel.2005.06.025.
56. Taylor MJ, Perrais D, Merrifield CJ. 2011. A high precision survey of the molecular dynamics of mammalian clathrin-mediated endocytosis. PLoS Biol 9:e1000604. https://doi.org/10.1371/journal.pbio.1000604.
57. Sherer NM, Lehmann MJ, Jimenez-Soto LF, Ingmundson A, Horner SM, Cicchetti G, Allen PG, Pypaert M, Cunningham JM, Mothes W. 2003. Visualization of retroviral replication in living cells reveals budding into multivesicular bodies. Traffic 4:785–801. https://doi.org/10.1034/j.1600-0854.2003.00135.x.
58. Tagawa A, Mezzacasa A, Hayer A, Longatti A, Pelkmans L, Helenius A. 2005. Assembly and trafficking of caveolar domains in the cell: caveolae as stable, cargo-triggered, vesicular transporters. J Cell Biol 170:769–779. https://doi.org/10.1083/jcb.200506103.
59. Habelhah H, Shah K, Huang L, Ostareck-Lederer A, Burlingame AL, Shokat KM, Hentze MW, Ronai Z. 2001. ERK phosphorylation drives cytoplasmic accumulation of hnRNP-K and inhibition of mRNA translation. Nat Cell Biol 3:325–330. https://doi.org/10.1038/35060131.